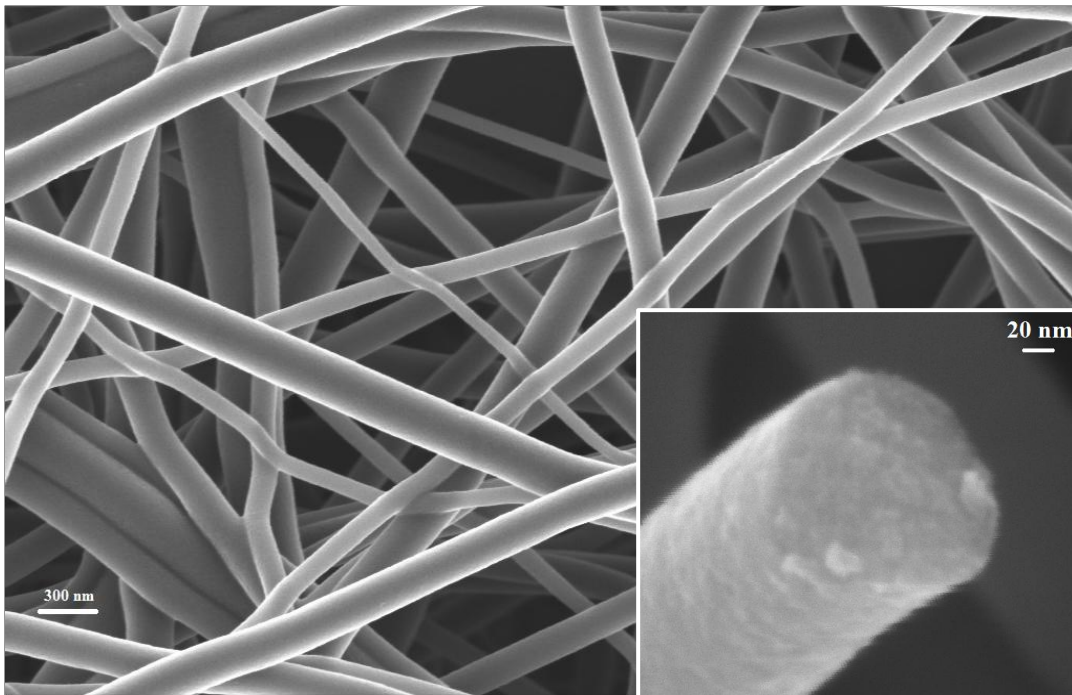# CHALMERS

Carbon nanofibers synthesized from electrospun cellulose

Master of Science Thesis in Materials and Nanotechnology

VOLODYMYR KUZMENKO

Department of Microtechnology and Nanoscience
CHALMERS UNIVERSITY OF TECHNOLOGY
Göteborg, Sweden, 2012

Carbon nanofibers synthesized from electrospun cellulose

VOLODYMYR KUZMENKO

Carbon nanofibers synthesized from electrospun cellulose
VOLODYMYR KUZMENKO

Department of Microtechnology and Nanoscience
Chalmers University of Technology
SE-412 96 Göteborg
Sweden
Telephone + 46 (0)31-772 1000

Cover: SEM images of carbon nanofibers
Göteborg, Sweden 2012

Carbon nanofibers synthesized from electrospun cellulose

VOLODYMYR KUZMENKO
Department of Microtechnology and Nanoscience
Chalmers University of Technology

SUMMARY

Carbon nanofibers (CNFs) have several properties that make them attractive for electronic devices, filtration membranes, tissue engineering scaffolds, composites (reinforcement agents), or catalyst carriers. Exploitation of renewable resources such as cellulosic materials can help to supply all these expanding demands.

Synthesis of carbon nanofibrous materials with controlled properties by carbonization of electrospun cellulose was performed in the present work. At the first step fine fibers were fabricated by electrospinning of cellulose acetate solution, they were subsequently regenerated to cellulose in various conditions and, finally, carbonized. Scanning electron microscopy (SEM) and x-ray diffraction (XRD) showed that carbonization of electrospun cellulose (EC) at 800 -1000 °C led to the formation of amorphous granular carbon nanofibers with diameters of 20-150 nm, controlled electrical conductivity (3.8 – 17.0 S/cm) and wettability (water contact angle is 55 – 120°).

Our analysis shows that the structure and properties of the resulting CNFs are influenced by deacetylation conditions and temperature of carbonization. XRD patterns illustrate different crystallinity indexes (CI) in different cases of deacetylation. Cellulose samples with sufficiently high CI are appropriate precursors for CNF synthesis.

Appended paper

Carbon nanofibers with controlled properties synthesized from electrospun cellulose.
O. Naboka, V. Kuzmenko, A. Sanz-Velasco, P. Lundgren, P. Enoksson, P. Gatenholm.
Carbon 2012, The Annual World Conference on Carbon, Krakow, Poland, June 17-22, 2012.

Table of contents

1. Introduction

In modern society advanced technologies have become an essential part of progress. No doubt, one of the biggest challenges is the development of novel materials with unique properties for various applications. In last decades a great deal of attention has been paid to nanomaterials that have proved to be very promising.

Carbon nanofibers (CNF) have several advantages that make them very attractive to researchers. CNF have exceptionally good mechanical and electrical properties; material made of them is relatively light and at the same time stiff and strong [1]. The valuable properties of CNF can be applied in a vast variety of ways, so the demand for this product is increasing continuously among the industrial consumers. They can be used as reinforcement agents in composites, templates, textile material, and as sieve in filtration. After some functionalization CNF are able to gain properties as an affinity membrane to collect proteins or a membrane that can recover metal ions. New tissue engineering scaffolds made of CNF are exploited in growing muscles, bones, cartilages, skin, blood vessels, neural tissues, etc. It is possible to heal wounds with CNF, deliver drugs with controllable release, they are efficient catalyst carriers for enhancement of catalytic reactions, and they have a great potential in sensors and electronic devices [2, 3, 4].

More than that, carbon is one of the main structural elements of organics in the universe. It is widely distributed in nature. Obviously, cellulose is the most available source of carbon, as this biomaterial can be found in plants where it serves as the dominant reinforcing phase in their structure, and it also appears in algae, and bacteria (Fig.1). Also in the form of different compounds Carbon is very abundant in the earth's crust including various coals and hydrocarbons [5, 6].
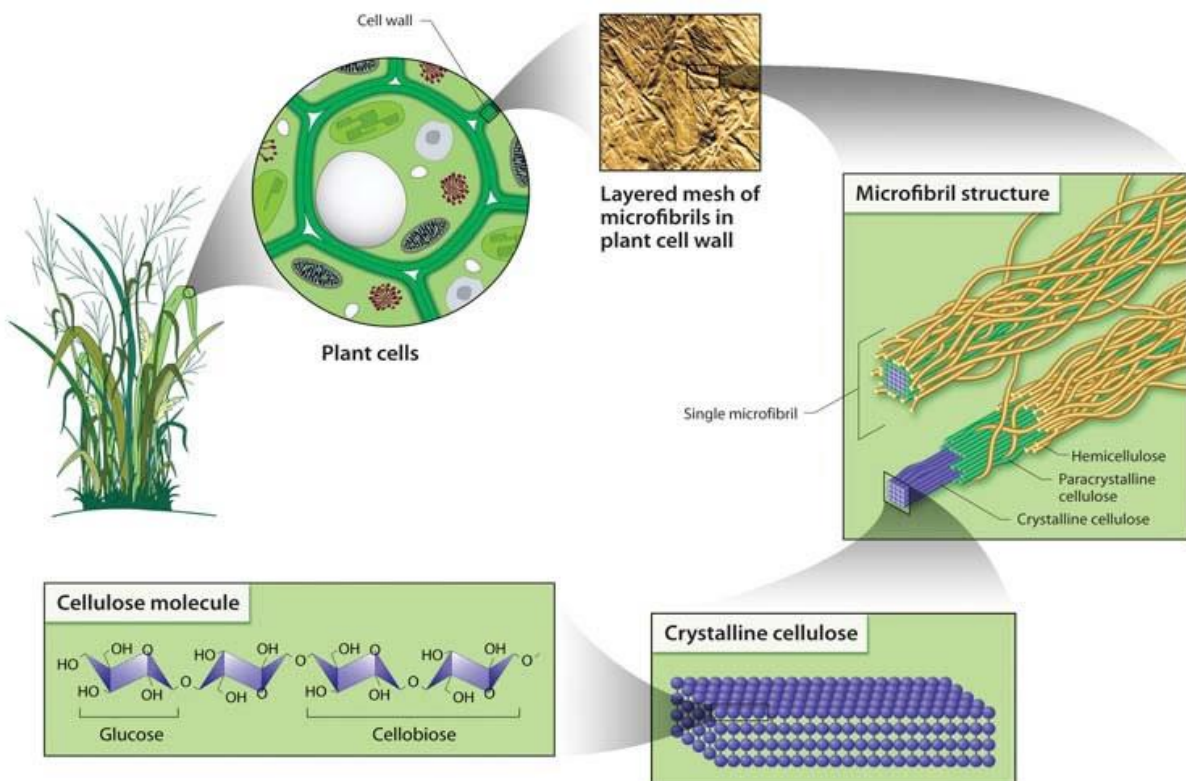

Figure 1: Cellulose structure at micro- and macrolevels
https://public.ornl.gov/site/gallery/originals/Fig2_Cellulose_Structure_a.jpg. 2012-05-02
genomicscience.energy.gov

1

There are different methods of CNF synthesis. The most common are thermal treatment of polymeric fibers and chemical vapor deposition (CVD). Other methods of CNF production are used only in laboratory scale [6].

One of the most promising methods of fiber preparation is electrospinning. On the contrary to such methods as template, self-assembly, phase separation, and melt-blowing, electrospinning allows obtaining continuous nanofibers on a large scale with easy adjustment of 1) the fiber diameter from nanometers to micrometers, 2) the orientation of the fibers, and 3) the distribution of different components in a structure [3, 4].

However there is one immense drawback of the present carbon materials production industry – deployment of resources of fossil origin. This is very important aspect as these resources are, firstly, extremely limited, and secondly, they cause emission of a large amount of greenhouse gases. That is why renewable sources can be a compromise solution to the problem of simultaneous improvement of the environmental performance of carbon products and sustainability maintenance in the world [7].

Cellulose as the most abundant renewable polymer is viewed to be a very prospective material for the production of CNF. Advantages of this biomass source are especially evident in the countries with valuable forest industry like Sweden or Canada. And no doubt, the trend of biomass utilization has a long-term life ahead of it [8].

1.1. Aim

The aim of this work is to conduct synthesis of carbon nanofibers (CNF) with controlled properties (such as conductivity and water contact angle) from cellulose through consecutive steps of: 1) CA electrospinning; 2) cellulose regeneration; 3) carbonization.

In particular attention is paid to deacetylation of cellulose acetate with the help of various methods and to the impact of these methods on cellulose crystallinity and subsequently on the properties of CNF.

2. Background

2.1. Carbon nanofibers

Today fibers occupy a big niche in the world market. The majority of them are still produced from such organic sources as cotton or wool, however the contribution of inorganic fibers increases continuously. Among the inorganic ones it is worth to put more emphasis on carbon fibers due to the opportunity of their utilization in different high-performance applications. The outstanding properties of carbon fibers are the main reason of the growing demand for them. Improvements in the production process result in the gradual decrease in cost (from $150 per pound in 1970 to less than $5 at the moment) [6, 9]

CNF are monomolecular carbon fibers with diameters ranging from tens of nanometers to several hundred nanometers, length range is 100 nm – 1000 µm. Carbon fibers with "nano" dimensions are very prospective as they have high specific surface area owing to their small diameters [2, 4]. The structure of CNF is different from carbon nanotubes (CNT) which are composed of one-atom-thick sheets of carbon (graphene sheets). Though CNF's mechanical and electrical properties are not as good as those of nanotubes, they possess one substantial advantage – they are relatively easy to synthesize with predetermined properties such as orientation, diameter, and distribution [1].

In this chapter synthesis and specific properties related to applications of carbon nanofibers are further overviewed.

2.1.1. Synthesis

There are two major approaches of carbon fibers production based on the precursor's state of matter: solid phase synthesis and vapor phase synthesis. The most used materials for the first one are polyacrylonitrile (PAN), pitch, and cellulose. Each one of them has several particular characteristics and advantages. The common feature for these precursors is their solid state at the initial stage of fabrication. Precursors are aligned into fibers through different spinning techniques, followed by stabilization and carbonization at temperatures up to about 1300 °C. Recently exploitation of a gaseous state of precursors has also gained its popularity. Vapor-grown carbon fibers (VGCF) are prepared by thermal decomposition or chemical vapor decomposition (CVD) of organic precursors, where stabilization is not necessary. While fibers from PAN, pitch and cellulosic precursors can be obtained as a continuous fibers with different morphologies (monofibers, strands of fibers, woven fabric with diverse woven modes, chopped fibers and also nonwoven mats), vapor-grown carbon fibers, on the other hand, are relatively short [6, 10].

PAN-based fibers represent the largest sector of the fiber manufacturing. These fibers have high tensile strength and modulus. The carbon content of acrylonitrile (CH_2=CHCN) of 67.9% together with its chemical structure result in a very high carbon yield of about 50–55%. In order to be suitable as precursor the acrylic fiber should contain at least 85% of acrylonitrile monomer to provide as high a carbon yield as possible; it should furthermore preserve the fibrous structure of the polymer precursor throughout the carbonization stage [9].

Pitch-based fibers are produced from low-cost by-products of the destructive distillation of coal, crude oil, or asphalt, and can be separated in two groups: the isotropic pitch fibers, which have low mechanical properties (Young's modulus is 35-70 GPa) and relatively cheap, and the mesophase pitch fibers, which have very high modulus (above 230 GPa) but are more

expensive. The carbon yield for the pitch-based fibers is even higher than for PAN-based – it can exceed 60% [6].

Generally, the synthesis of high-performance (HP) carbon fibers from PAN and pitch precursors takes 4 steps as shown at Figure 2. At first stage fibers are formed by spinning process. During spinning the fibers are also stretched which gives them higher strength because of parallel orientation of fiber axes. Stretching can be performed after spinning separately as well. Afterwards stretched fibers are stabilized by slow heating at 200-400 °C in an O_2-containing atmosphere to avoid detrimental chain scission, fusion of fibers, and relaxation of the fibrillar construction during further carbonization by enhancing oxidation cross-linking of the structure. Carbonization is done at 1200-1400 °C in inert atmosphere for PAN-based fibers and at 800-1200 °C for pitch-based fibers (with slow heating rate to avoid prompt gas evolution). Such volatile by-products as H_2O, CO_2, CO, NH_3, and HCN are released leaving just carbon. At this stage general performance (GP) fibers are made. The tensile modulus of the fiber can be further increased by heat treatment at 2000-3000 °C to get HP fibers with improved properties [6, 10].

Precursor (PAN or pitch)
• Spinning

Fibers
• Stabilization in air (200-400 °C)

Stabilized fibers
• Carbonization in inert atm (800-1400 °C)

GP-grade carbon fibers
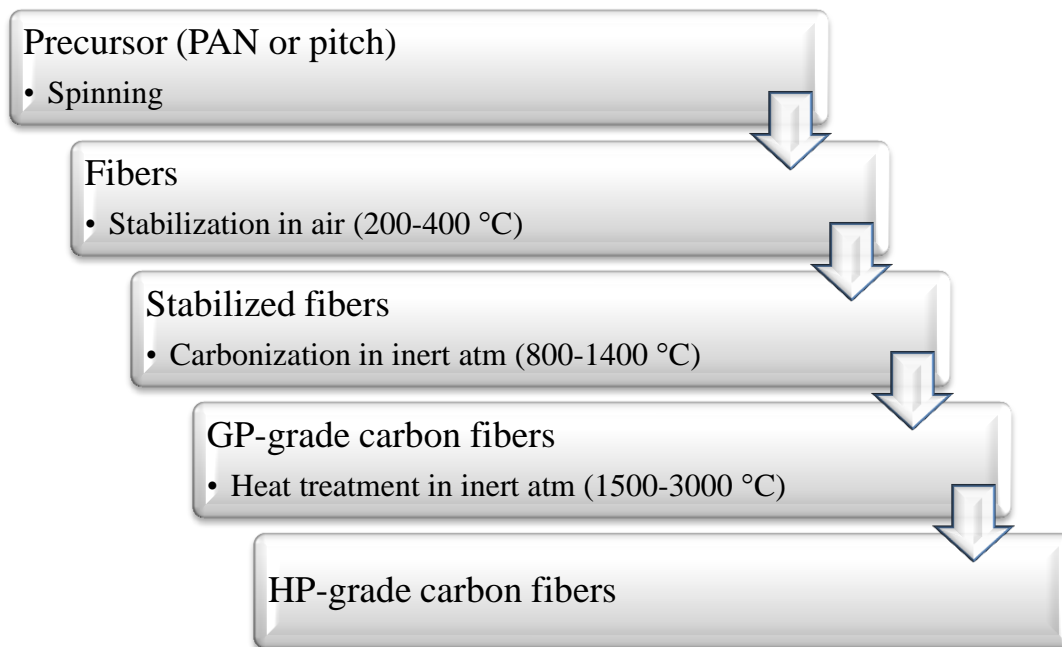• Heat treatment in inert atm (1500-3000 °C)

HP-grade carbon fibers

Figure 2: Production procedure for PAN- and pitch-based carbon fibers [10]

Cellulose-based fibers were developed in the 1960's for aerospace applications and became at that time the first carbon fibers produced commercially [6]. Though they are not as strong as PAN-based fibers they have a huge advantage – abundant resources of the precursor. In Ch. 2.2 cellulose-based fibers are overviewed in more details.

Vapor-phase fibers still require a lot of development, but even now their potential seems very promising. VGCF are prepared by the catalytic decomposition of a carbon precursor (usually hydrocarbon gas) in two different ways depending of the catalyst positioning (Fig. 3). In the seeding catalyst method, catalyst particles are seeded on a substrate, such as graphite or ceramics, while in the floating catalyst method catalyst is fed continuously to the reaction space giving higher fiber yield as a result. In both methods pre-activated with high-purity hydrogen gas catalytic particles (Fe, Ni, Co, iron metallo-organics like ferrocene $(C_5H_5)_2Fe$, etc.) with a size of sub-100 nm are applied. Substrate temperature, plasma power, and chamber pressure are the three main growth parameters. The temperature needed for fiber

growth has to be at least 600 °C, the growth rate is close to 1 mm/min in length and diameter range is extremely broad – from 100 nm to 10 μm. Vapor-phase fibers have high tensile strength, diameters of 0.5-2 μm, but cannot be longer than 50 mm. This feature makes them very much fit for different composites as reinforcement agents [6, 10, 11].
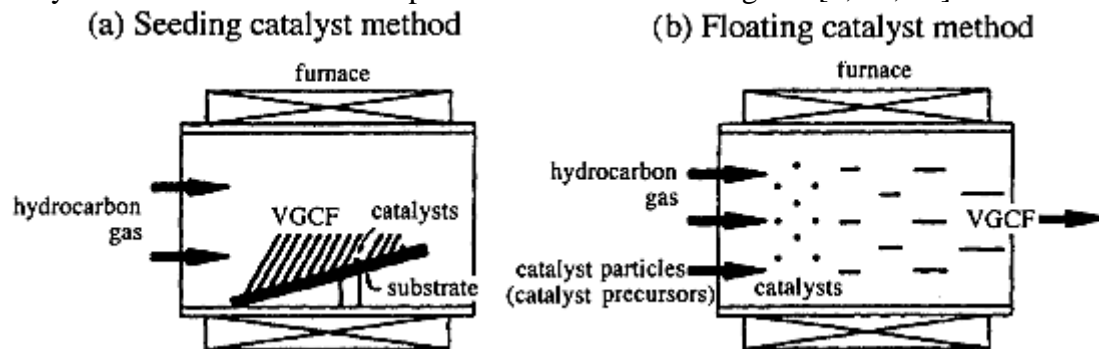

Figure 3: Two methods of VGCF fiber production [10]

2.1.2. Properties and applications

The main reason of the recent popularity of nanotechnology is that the reduction of the dimensions of a material to nano-size leads to new specific properties [2]. Carbon nanofibers have very high tensile strength and Young's modulus (can reach values of about 12,000 MPa and 600 GPa respectively) which are approximately 10 times that of steel. Besides mechanical strength, CNF are attractive in electrical applications as well due to their high electrical conductivity. These properties of CNF give a huge number of opportunities of their future applications in all spheres of life [12].

The large surface area of a porous nanofibrous material can be used in *energy conversion and storage*. Most of the batteries nowadays use sponge-like electrode with high discharge current and capacity, and a porous separator between the electrodes which can prevent short circuit and allow free exchange of ions (Fig. 4). Nanofibers with well interconnected pores, high mechanical strength and electrochemical stability seem very suitable for porous separators. They sustain a substantial uptake of electrolyte solution and enable high ion conductivity. Also CNF can be used as battery electrodes to improve reversible capacity (long life-time when cycling) or as hydrogen-storage material [4].
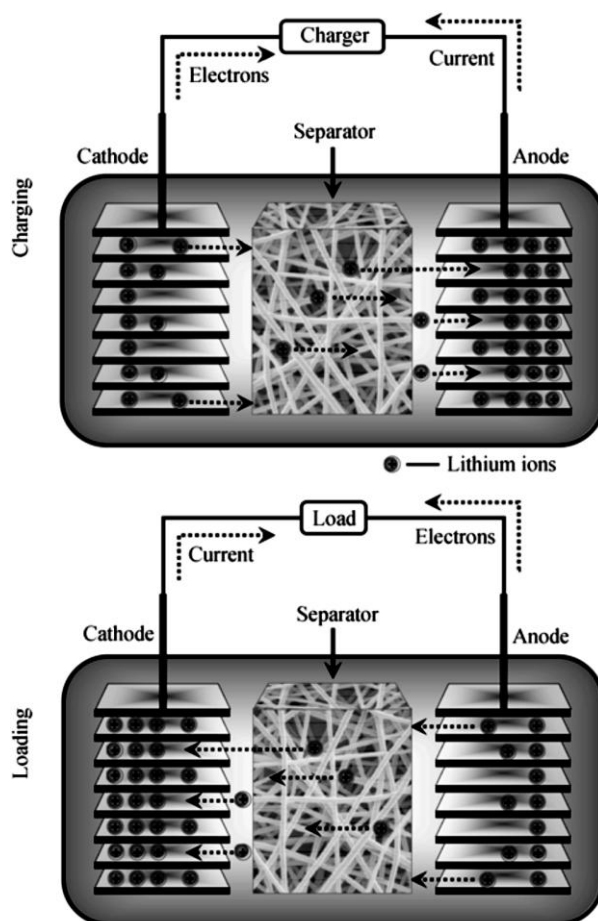
Figure 4: Charging and discharging processes in a lithium ion battery [4]

The superb mechanical properties of CNF make them a good *reinforcement* agent for different synthetic materials. In comparison with macroscopic fibers, a lower quantity of nanofibers is required to attain the same reinforcement result and reduce brittleness; their large specific surface area promotes relaxation processes in the matrix as well, which improves the impact strength of the reinforced matrix. More than that, the small diameters of CNF provide very limited refraction of light which makes them transparent in matrices [2].

The large surface area and chemical inertness of CNF can be applied in *catalysis*. For example, nanofibers loaded with metallic nanoparticles (Rh, Pt, Pd) are appropriate catalyst carriers for hydrogenation reactions. The elimination and recycling of the catalyst after the reaction is not a problem, nanofibers are very effective in the terms of time and conversion, and they can serve several times without loss of activity [2].

CNF have also found their way into the *medical field*. The reason is that the dimensions of proteins, viruses, and bacteria belong to the nanoscale size range. At the moment, vivid examples of this phenomenon can be observed in tissue engineering. Impalefection, a method of gene delivery, uses CNF to attach plasmid DNA containing the gene that is intended for entering the cell. Then this gene-activated matrix is pressed against cells or tissue causing the subsequent gene expression [13]. The similarity in dimensions of CNF compared to crystalline hydroxyapatite found in bone, as well as its high strength to weight ratio, can make it applicable as an orthopedic/dental implant material [14].

Membranes made of CNF can be an efficient tool for *filtration* providing a rather insignificant decrease in permeability and a higher capability to trap fine particles compared to

conventional filter fibers. The adsorption of particles is determined by the sieve effect for large particles and by static electrical attraction for particles smaller than the pores. It is a suitable method to collect airborne particles in the wide diameter range of 0.5-200 μm [4].

2.2. Cellulose as precursor for synthesis of CNF

In order to produce carbon fibers a precursor should be easily converted to carbon at as high a yield as possible to be economically viable. A cellulosic precursor $(C_6H_{10}O_5)_n$ has an initial carbon content of 44.4% which enables carbon yields of about 10-15% [10].

Figure 5 shows the common scheme of CNF synthesis from cellulosic precursors. At the first step the cellulosic precursor (usually CA) is spun to produce a fibrillar structure [15]. This structure remains intact during the cellulose regeneration process and carbonization, except for the initial diameter decrease of about 3-4 times due to carbonization [9]. The most appropriate method of fiber spinning, i.e. electrospinning, regeneration of cellulose and carbonization are described below in this chapter.

Cellulosic precursor
• Spinning

Cellulose derivative fibers
• Regeneration

Cellulose fibers
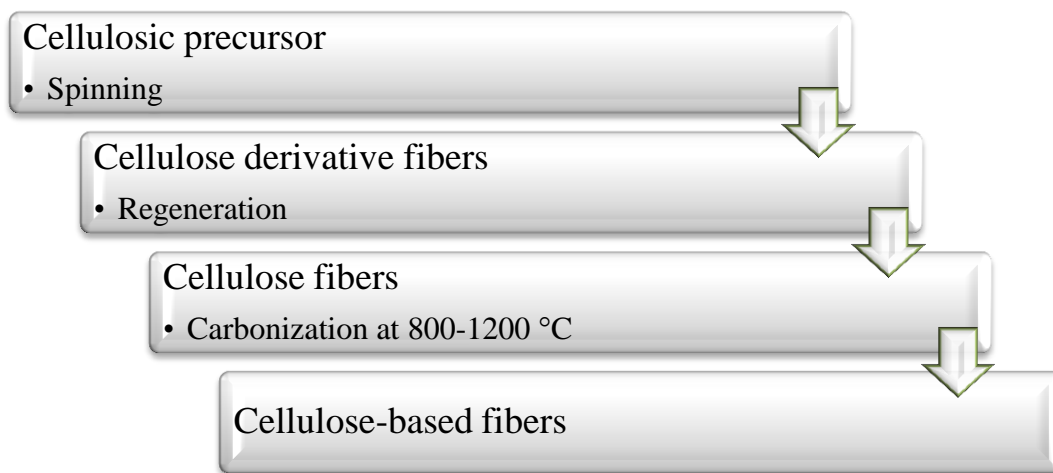• Carbonization at 800-1200 °C

Cellulose-based fibers

Figure 5: Production procedure for cellulose-based carbon fibers [9]

2.2.1. Structure of cellulose and its derivatives

Cellulose is a naturally occurring polysaccharide that consists of D-glucose monomer units joined by 1–4 glucosidic bonds, forming an ether linkage by the elimination of water (one molecule may include up to ten thousand units). These ether linkages together with hydrogen bonds between different units make cellulose relatively stiff and hard to dissolve (Fig. 6). It is not soluble in the most common solvents, which leads to extremely difficult processing of cellulose. On the other hand, its derivatives are much easier to handle (using different modifications) with spinning processes [9, 16].
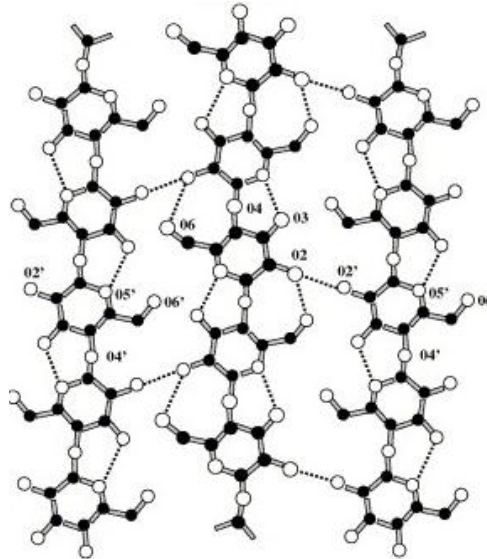
Figure 6: The chemical structure of cellulose with possible intra- and intermolecular hydrogen bonds [17]

Cellulose acetates are common esters of cellulose. They are synthesized by a reaction of cellulose with acetic anhydride or acetic acid in the presence of sulfuric acid. The degree of substitution (DS) of hydroxyls on acetic groups in cellulose may vary from 0 to 3 (Fig. 7), the range of 2-2.5 is predominantly used [18].
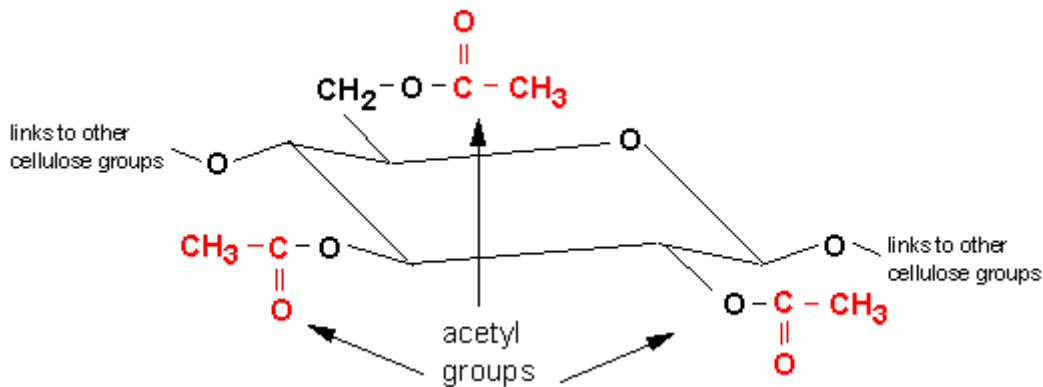

Figure 7: The chemical structure of cellulose triacetate
http://nfsa.gov.au/site_media/uploads/images/2010/08/23/acetateformula.gif 2012-03-15

DS affects the solubility of CA and hence determines the options for further processing for different applications. For example, CA with DS of 2 – 2.5 is soluble in such solvents as acetone, dioxane or methyl acetate, while celluloses with higher degree of acetylation are soluble in dichloromethane. Generally, acetylation makes cellulose more soluble in organic solvents, so it makes more suitable then to produce films from cellulose triacetate (the easiest one to dissolve), membranes and fibers from cellulose 2–2.5-acetate [18].

2.2.2. Regeneration of cellulose

On the contrary to cellulose, CA is a thermoplastic material, which starts to destruct at temperatures about 200 °C, far below carbonization of the composition [19]. It makes CA fibers impossible to use as they do not keep their structure. That is why the regeneration step is a very pivotal one in CNF production since it converts cellulose derivatives back to cellulose, thus creating a proper precursor for carbonization. The distinctive property of cellulose to decompose before it melts is the main reason for that [9].

The treatment of cellulose esters in alkaline solutions leads to the removal of the carboxylic groups and the regeneration of cellulose. The hydrolysis of carboxylic esters catalyzed by alkali agents in liquid solution takes place via a three-step process as it is shown in the example of cellulose acetate in Figure 8. In the first step, the negative ion RO^- (R is usually hydrogen atom if alkali bases are used) from the base regenerative agent attacks the ester carbon creating delocalized negative charge between oxygen atoms. This step is reversible and the slowest one, which means that it determines the overall rate of cellulose regeneration. The other two steps are fast and irreversible resulting in acetic acid and alcohol as the products. At the end, the acetate groups of cellulose acetate turn into cellulose-OH by hydrogen abstraction [16].
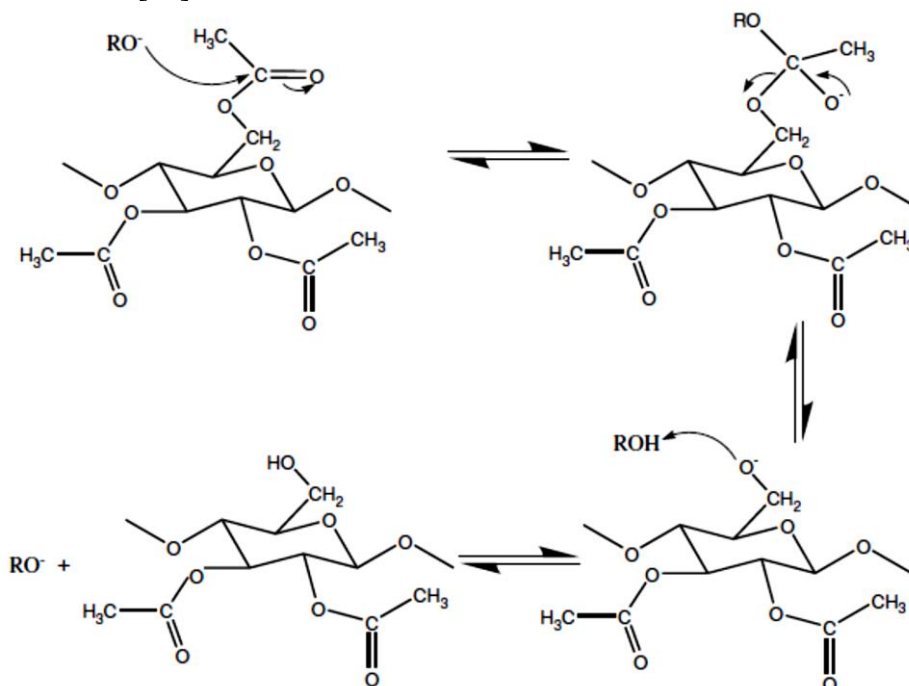

Figure 8: Cellulose deacetylation [16]

2.2.3. Carbonization

General information

Carbonization is the transformation of the organic precursor into a material that contains predominantly carbon. The precursor is heated in a reducing or inert environment. The temperatures may vary depending on the nature of the particular precursor, sometimes extending to 1300 °C. As the result, after the complex process that includes different reactions the initial organic material turns into a valuable carbon residue, while volatile compounds diffuse out of the system. The carbon content of this residue differs depending on the nature of the precursor and the pyrolysis temperature, but usually stays in the range 90 to 99 wt% [6].

Another important aspect of carbonization is the carbon yield, which is the ratio between the weights of the carbon material after and before carbonization. The yield is influenced by the heating rate, the carbonization atmosphere, and the pressure. Typically carbon yield does not exceed 60% [6].

In order to avoid disruption and rupture of the carbon network the diffusion of volatile compounds should be slow. The duration of carbonization depends on the desired structure of

the product, the type of precursor, and the thickness of the material. For example, production of large electrodes requires several weeks, while carbon fibers can be fabricated relatively fast due to their small cross-section that makes diffusion paths shorter [6].

At the end of carbonization "amorphous carbon" is typically obtained. X-ray diffraction shows that it lacks long-range crystalline order and the deviation of the interatomic distances of the carbon atoms from the perfect graphite crystal is more than 5% in both the basal plane and between planes [6]. To obtain a more ordered structure of carbon (graphitizing carbon) carbonization should be conducted at higher pressures or with the use of a catalyst [20].

Carbonization of cellulose
Cellulose is one of the oldest polymer precursors used in the production of fibers. Generally polymers have a lower carbon yield compared to aromatic hydrocarbons since, except carbon and hydrogen, they contain elements like oxygen, chlorine, or nitrogen that must be removed during pyrolysis. Cellulose gives a carbon yield at about 20% [9].
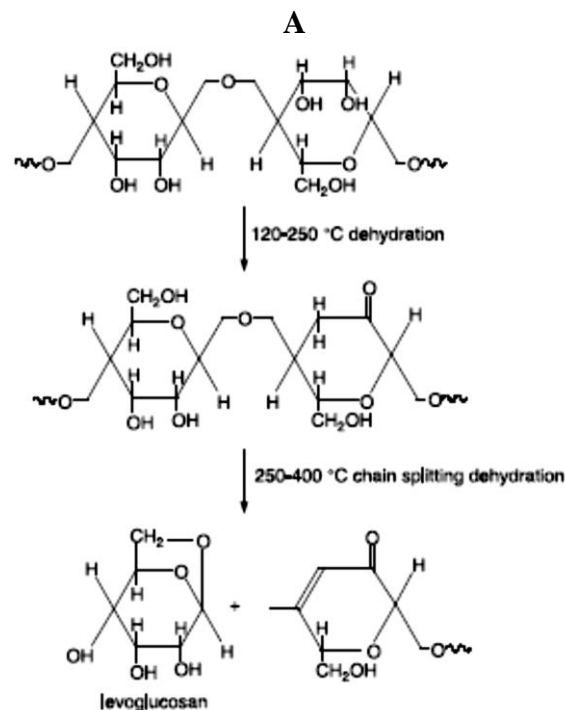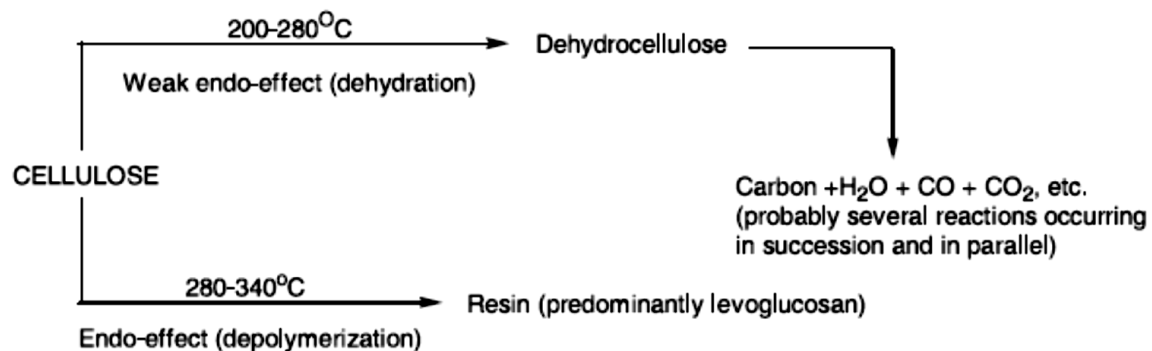
A

B

Figure 9: A. The scheme of cellulose decomposition during the carbonization cycle (two possible ways are shown); B. Changes in chemical structure of cellulose during the first stages of carbonization cycle [9]

During pyrolysis and carbonization the cellulosic precursor continuously releases some compounds. At the first stage absorbed water is lost at temperatures up to about 120 °C, after that a dehydration process occurs up to 300 °C resulting in dehydrocellulose (Fig. 9). At about 250 °C simultaneously with dehydration cellulose starts to depolymerize mostly forming 1,6-anhydro-b-D-glucopyranose (levoglucosan). This chain-splitting reaction is not desirable since it lowers the yield, so holding the temperature at the beginning of carbonization below 250 °C for few hours can be an efficient way to produce carbon fibers. At the last stage highly volatile gases, a tarry distillate and a carbon char are formed [6, 9].

2.3. Electrospinning as a prospective method of fiber production

Electrospinning is the most flexible and easily controlled process of nanofibers production nowadays. It has several important advantages compared to other methods (melt-spinning, dry-spinning, template synthesis, self-assembly, phase separation). First of all, electrospinning allows obtaining continuous nanofibers with desired properties in a relatively simple and fast way. Secondly, a large variety of fiber assemblies (nonwoven, aligned, patterned etc.) and fiber diameters (from 3 nm and up to around 10 μm) is possible to get by simple changes in the process parameters. Thirdly, the produced fibers have an extremely high surface-to-mass ratio due to a developed porous structure. Finally, electrospinning gives the opportunity to fabricate nanofibers from completely different materials such as polymers, metals, ceramics, or to combine them to form composites [4, 21, 22].

2.3.1. Basic principles

The electrospinning process is based on the uniaxial stretching of a viscoelastic solution by electrostatic forces. Continuous fiber formation takes place as long as the solution keeps on feeding the electrospinning jet. The whole set-up for electrospinning includes a high voltage source (up to 30 kV), a solution container with milliliter size capillary (e.g. a syringe with a flat tip needle), and a conducting collector (Fig. 10). The solution is usually fed through a positively charged spinneret with the help of a pump. When it comes out of the needle tip a high voltage is required to form a jet shooting towards a collector. Once the electric field reaches a critical value at which the repulsive electric force overcomes the surface tension of polymer solution, the polymer solution is ejected from the tip to the collector. Strong electrostatic forces make the solution jet come out from the needle to form a so-called Taylor cone and subsequently stretch into thin fibers in the direction of the grounded collector. As a result, while the solvent evaporates solid fibers are collected to produce a nonwoven fibrous mat [4, 21, 23, 24, 25].
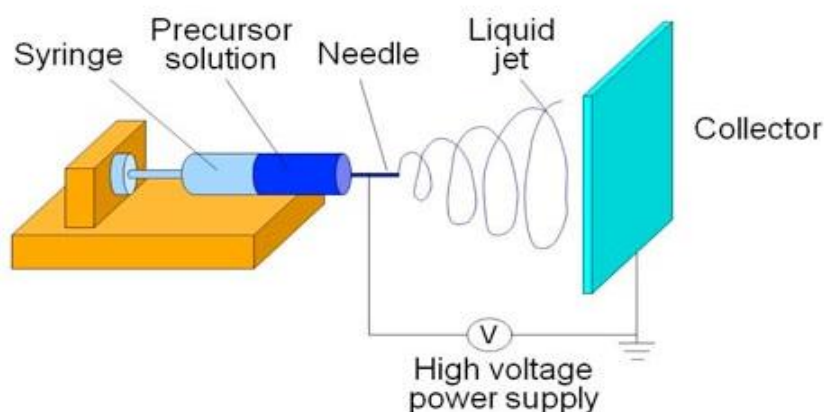

Figure 10: Electrospinning setup
http://images.iop.org/objects/ntw/journal/8/4/9/image2.jpg 2011-11-13

11

2.3.2. Parameters

The most important parameters that influence the electrospinning process can be divided into three main categories: 1) solution properties (including viscosity of solution or concentration, solution charge density, surface tension, polymer molecular weight, dipole moment, and dielectric constant); 2) controlled variables (applied voltage, distance from spinneret tip to collector, flow rate, collector and needle tip design); 3) ambient factors (temperature, humidity, air velocity). Obviously, it is impossible to isolate the effect of many of the parameters because they all are interrelated. The best way to obtain uniform, smooth fibers is to try spinning at varied parameters until perfection is reached [23, 26]. The effects of electrospinning parameters on fiber size and morphology are described below.

Solution properties

The polymer concentration is directly proportional to the *solution viscosity*, which has the biggest influence on the size and morphology of electrospun fibers. Previous experience of polymer electrospinning shows that a lower concentration leads to the formation of defects such as beads and droplets since the viscosity is too low to create a strong thin fiber (Fig. 11). As a result, the solution is not sufficiently stretched to the collector, but rather sprayed onto it [27, 28, 29, 30]. It also allows some solvent to get to collector and cause wet fibers to form junctions and bundles [28]. Increasing the solution viscosity significantly reduces these defects, producing fibers which are more uniform. However, a too viscous solution is impossible to electrospin due to clogging of the needle tip (solvent evaporates faster than jet is initiated) [30, 31]. The diameter of the electrospun fiber correlates to the polymer concentration as well. A higher viscosity of the solution results in thicker fibers [4, 28, 32, 33]. A higher *solution conductivity* or *charge density* generally helps to produce more uniform fibers with fewer defects [29, 31, 34, 35]. The conductivity can be increased by addition of a volatile salt (it would not stay in the end product), alcohol [36], or a surfactant [37].
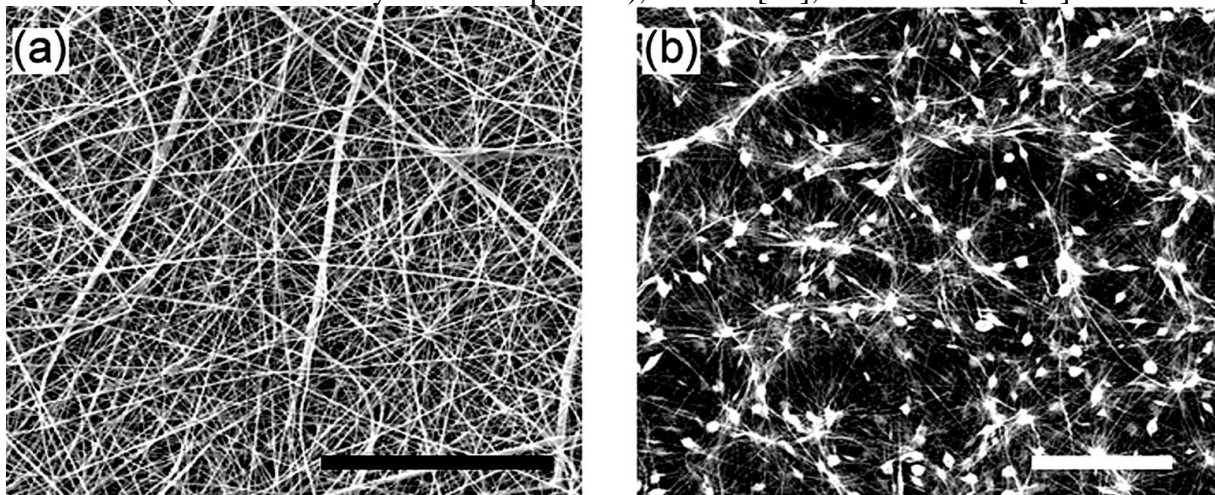

Figure 11: a) Example of uniform fibers; b) Example of fibers with defects (beads) [26]

Controlled variables

The applied voltage has a significant impact on the fiber fine structure. First and most important of all, the electric field must be strong enough to overcome the surface tension in order to induce spinning. On the other hand, spinning at as low voltage as possible is desirable for the production bead-free fibers. In this case the Taylor cone is formed at the needle tip followed by smooth stretching of the solution. Higher voltages lead to a jet originating from the liquid surface within the tip (without the Taylor cone being formed) resulting in beading. A further increase in the electric field can even split jet into several [28, 30, 31]. The *flow rate*

indicates the speed at which the solution is fed to the needle tip. Different studies prove that lower flow rates allow obtaining uniform fibers with smaller diameter [31], while higher flow rates yield beaded fibers due to solvent inability to evaporate before reaching the collector [36, 38]. *The distance between the tip and the collector* (distance between two electrodes) should be sufficient to let the fibers dry before reaching their final destination. The distance also affects the shape and diameter of the obtained fibers. The most suitable distance has to be found experimentally for each electrospinning setup [4, 39]. *The designs of the needle tip and the collector* also play important roles in electrospinning. Their huge diversity nowadays allows getting fibers with absolutely unique structures. For example, coaxial spinning with a two-capillary spinneret makes it possible to produce hollow fibers [40], spinnerets with multiple tips can produce fibers with various weight ratios of blended polymers with a controlled distribution [41]. Metal collectors with conductive surfaces generally help to form fibers with uniform structure without any shrinking or swelling [42]. Non-conductive collectors cause repulsion between the fibers resulting in lower packing density [33]. Versatile geometries of collectors bring electrospinning to a new level. Obtained fibers can have different alignment, wide range of diameters and assemblies [43, 44, 45].

Ambient factors
Some previous investigations show that the fiber diameter is inversely proportional to *temperature*. It can be explained by a correlation between temperature and the viscosity of a solution [35]. Increasing the *humidity* results in the appearance of small circular pores on the surface of the fibers [46].

2.3.3. Electrospinning of cellulose acetate (CA)
Electrospinning of polysaccharides is not an easy task to accomplish because of their poor solubility and the high surface tension of solutions [47]. Cellulose gives a vivid example of it. Solvents that can dissolve this polysaccharide have low volatility and high melting temperature, which makes it hard to remove them completely from the fibers and requires electrospinning to be performed at relatively high temperatures [48, 49, 50, 51, 52].

Cellulose acetate is a cellulose derivative that is much easier to handle which makes it favorable in electrospinning processes. In order to choose a good solvent several factors should be taken into consideration. First of all, the solvent must have a high enough boiling point and dipole moment in order to evaporate during the stretching of the fibers towards the collector and not before. Otherwise clogging of the needle tip is observed. Secondly, the resulting solution should not be too viscous, but it should have high conductivity and low surface tension [15, 53, 54,]. That is why the presence of solvents with a high dielectric constant and boiling point like dimethylacetamide, methanol, dimethylformamide or water improves the spinnability of CA solutions. Usually they are mixed with low-boiling solvents (acetone, chloroform, dichloromethane) in different weight ratios to obtain the best suitable solvent for a particular molecular weight of CA and a target structure. After getting cellulose acetate fibers they are regenerated to cellulose by aqueous or ethanolic hydrolysis [47].

4. Materials and methods

4.1. Materials

Acetone (99.9%, Sigma Aldrich), dimethylacetamide (DMAc, 99.9%, Sigma Aldrich), cellulose acetate (CA, Mn = 30,000, 39.8% acetyl groups, Sigma Aldrich), sodium hydroxide (NaOH, Sigma Aldrich), ethanol (95%, Solveco), deionized water (DI H_2O), and ammonium hydroxide (NH_4OH, 28%, Sigma Aldrich) were used without additional purification.

4.2. Electrospinning

1.7 g of CA was dissolved in 10 ml of the solvent mixture of acetone and DMAc (volume ratio 2:1) at room temperature. The prepared solution was kept in a tightly closed bottle overnight before electrospinning. For electrospinning CA solution was transferred to a 10 ml disposable syringe and then fed continuously by the syringe pump (Harvard Apparatus) at a flow rate of 1 ml/h through a stainless steel needle with a flat tip (Howard Electronic Instruments Inc.). The inner diameter of needle was 0.643 mm (Fig. 12).
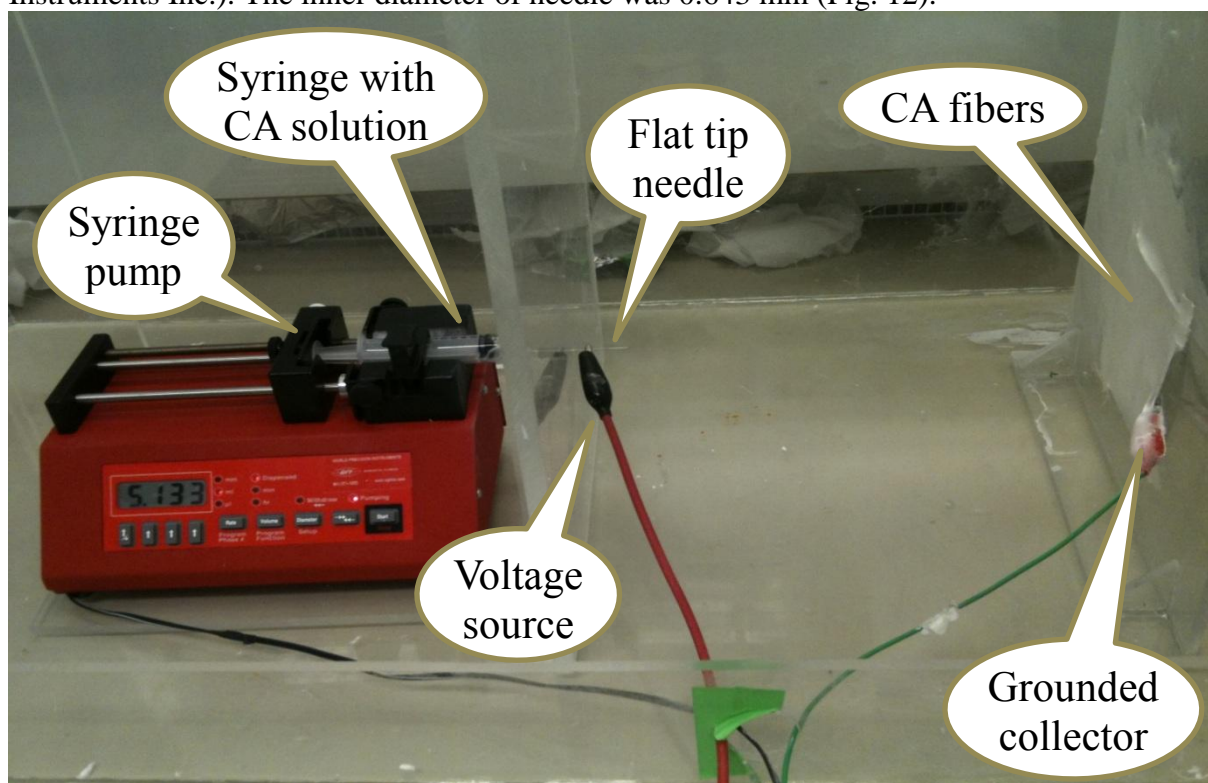

Figure 12: Syringe pump, 10 ml syringe and needle with a flat tip

The steel needle was connected to a high voltage supply (Spellman's CZE1000R) with a positively charged electrode. The grounded collector (10 cm × 10 cm steel mesh covered tightly with aluminum foil) was connected to negatively charged electrode. The voltage between needle and collector was 25 kV, the distance – 25 cm, and the collection setup was horizontal. Ambient conditions: temperature around 20 °C, relative humidity (RH) from 45 to 60% (when air was too dry humidity was kept in this range artificially with the help of a humidifier). The amount of electrospun CA solution was around 2 ml for one sample.

4.3. Deacetylation of cellulose acetate to produce cellulose

Electrospun cellulose acetate mats were left on the aluminum foil under the fume hood for at least 24 hours to let all the remaining solvents evaporate before further treatment. Then the

dried cellulose samples were peeled off from the foil and cut into 4 pieces of about the same size (5 cm × 5 cm).

4.3.1. Deacetylation with NH₄OH

Table 1: Conditions of cellulose regeneration with NH₄OH

Sample number	Regeneration agent	Concentration	Additional component	Time
I				4 days
II			ethanol	
III	NH$_4$OH	28%		8 days
IV			ethanol	
V				14 days
VI			ethanol	

Cellulose acetate samples were immersed into two different solutions in the plastic beakers: pure 28% NH$_4$OH solution (100 ml) and 28% NH$_4$OH solution (100 ml) with addition of ethanol (5 ml). They were left at room temperature for 4, 8 or 14 days in order to regenerate cellulose. They were then washed from NH$_4$OH solution by DI water several times (up to 8) until neutral pH was reached. The drying procedure was identical to the one mentioned above.

4.3.2. Deacetylation with NaOH

Table 2: Conditions of cellulose regeneration with NaOH

Sample number	Regeneration agent	Concentration	Solvent	Time
VII		0.05 M	ethanol	
VIII	NaOH		water	24 h
IX		0.1 M	ethanol	
X			water	
XI	NaOH + NaCl	3.75 M + 2.1 M	water	40 min

Ethanol solution
Cellulose acetate samples were immersed into 0.05 M or 0.1 M NaOH solution in ethanol in the plastic beakers (100 ml) and left for 24 hours at room temperature in order to regenerate cellulose. Then all the samples were rinsed up to 8 times with DI water to remove NaOH (until pH reached 7). Some samples were also additionally treated after the first regeneration. They were put into water bath at 70 °C for 1 hour.

After the regeneration procedure was completed all samples were spread inside the PS Petri dishes for drying. EC was left drying at room temperature (RT) in Petri dishes with the lid slightly open.

Water solution
Cellulose acetate samples were immersed into 0.05 M or 0.1 M NaOH solution in water in the plastic beakers (100 ml) and left for one day at room temperature in order to regenerate cellulose. The day after all the samples were rinsed up to 8 times with DI water to stop the

reaction and to remove NaOH, and kept in water until further treatment (pH was checked to be sure about NaOH removal). The drying procedure was identical to the previous one.

4.4. Carbonization of cellulose mats to synthesize carbon nanofibers

Cellulose samples were placed into the tube furnace with inert N_2 atmosphere (flow of gas was 1 l/min) between two silicon wafers. Temperature was raised with rate of 5 °C/min up to 800 or 1000 °C and was held there for 2 hours. After that the furnace was switched off, and the samples were left in the oven until the temperature inside reached room temperature.

4.5. Characterization

After the regeneration procedure the dried samples were analyzed with Fourier-transform infrared (FTIR) spectroscopy, scanning electron microscopy (SEM), and x-ray powder diffraction (XRD) to get information about the degree of regeneration of cellulose, the morphology of the regenerated cellulose fibers, and the crystalline structure respectively.

After the carbonization CNF were analyzed with x-ray photoelectron spectroscopy (XPS), energy-dispersive X-ray spectroscopy (EDS), scanning electron microscopy (SEM), x-ray powder diffraction (XRD), thermal gravimetric analysis (TGA), four-point probe method, and contact angle measurements to get information about the chemical and elemental composition, morphology, crystalline structure, decomposition behavior during carbonization process, conductivity, and wettability respectively.

4.5.1. SEM and EDS

Electrospun cellulose acetate samples, regenerated samples of cellulose, and carbon nanofibers were analyzed with SEM (Zeiss Leo Ultra 55 FEG SEM) to investigate the changes in morphology caused by deacetylation treatment.

Energy dispersive X-Ray microanalysis (EDX) was performed with Oxford Inca EDX system at 5.0 kV.

4.5.2. FTIR spectroscopy

Experimental solid samples for FTIR spectra were obtained by making pellets of 100 mg weight with weight ratio KBr/sample = 200/1. FTIR spectroscopic analysis (Perkin Elmer System 2000 FT-IR) was set on transmission mode; wavenumber range was in between 370 and 4000 cm^{-1}, resolution of scanning – 4 cm^{-1}, number of scans – 20.

4.5.3. XRD

The crystalline structure of the regenerated cellulose samples and carbon nanofibers was examined by the XRD method (Philips X'Pert Materials Research Diffractometer (MRD)) performing at 2θ values of 10–37° (for cellulose) and X-Y (for CNF) with resolution of 0.05°, averaging time per step was 30 s. The source of radiation was an X-ray tube with Cu anode (Kα radiation, λ=1.54184 Å) at 45 kV and 40 mA. Phase analysis was executed with X'Pert HighScore 3.0 (PANalytical BV) using ICDD databases (release 2008/2009).

In our work an empirical equation is used to determine the crystallinity index (CI) of the cellulose samples: $CI\% = 100(I_{max}-I_{min})/I_{max}$, where I_{max} is the scattered intensity of the main peak for the regenerated cellulose at maximum (2θ = 18-22°), and I_{min} is the scattered intensity at the minimum (2θ = 13-15°) [55].

16

4.5.4. TGA

This analysis was performed with Pyris TGA 7 (Perkin Elmer). Samples of the regenerated cellulose were placed into the tube oven for TGA with inert N_2 atmosphere (flow of gas was 20 ml/min) inside the platinum sample pan; they were covered with a silicon wafer in order to simulate carbonization conditions. First the temperature was held at 105 °C for 30 min to remove physically adsorbed water. Then it was raised with a heating rate of 5 °C/min up to 800 °C and was held there for 30 minutes.

4.5.5. XPS

XPS was performed with the Quantum 2000 scanning ESCA microprobe from Physical Electronics. An Al Kα (1486.6 eV) X-ray source was used and the beam size was 100 μm. The analyzed area was approximately 500 x 500 $μm^2$.

4.5.6. Four-point probe

The electrical conductivity measurements were performed using a four-point probe system (CMT-SR2000N, AIT).

4.5.7. Contact angle measurement

Contact angle measurements were carried out by the sessile droplet technique (10 μm droplet volume) with VCA 2500 (Video Contact Angle System), AST Inc. (Advanced Surface Technology Inc.).

5. Results and discussion

White flexible fibrous mats with thicknesses of about 60-90 μm were received via electrospinning of CA solution (Fig. 13). The diameter of the fibers was 0.3-1.5 μm. Afterwards they were hydrolyzed with different methods in order to get a fibrous cellulosic precursor for carbonization process.
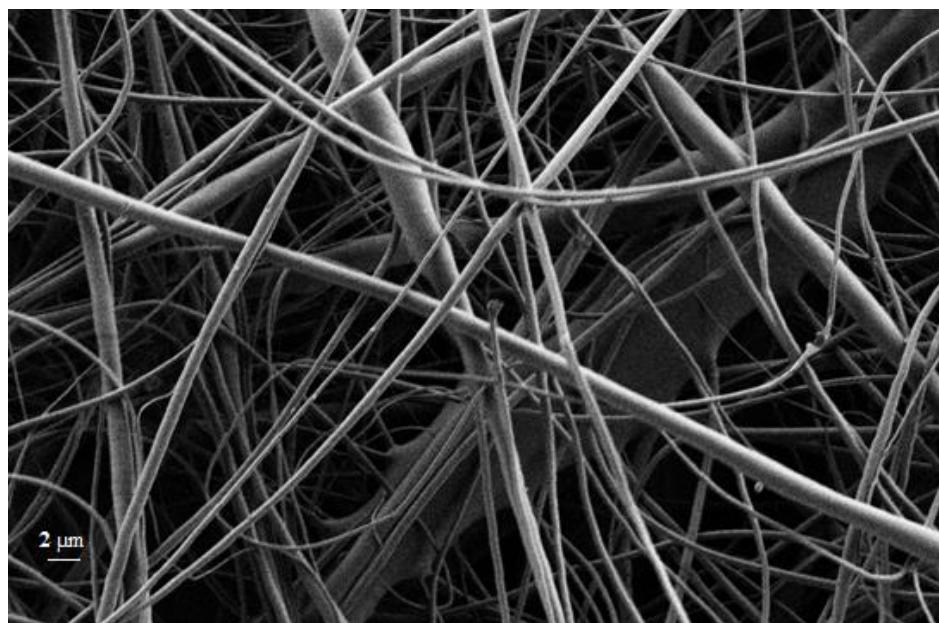

Figure 13: SEM picture of electrospun CA fibers

5.1. Regenerated cellulose

5.1.1. Morphology

According to SEM analysis samples regenerated with 0.05-1 M NaOH (VII-X) and with NH_4OH (I-VI) have retained the morphology of the starting electrospun EC (Fig. 14A-B), which is consistent with previous experience [33]. The resulting fibers have diameters of about 0.3-1.5 μm (Fig. 14B). In the case of the cellulose regeneration with highly concentrated NaOH and NaCl (XI) the fibers get deformed (Fig. 14C). A possible reason for this effect could be significant swelling of the cellulose which would lead to the loss in the degree of fiber orientation and deformation as a result [56].
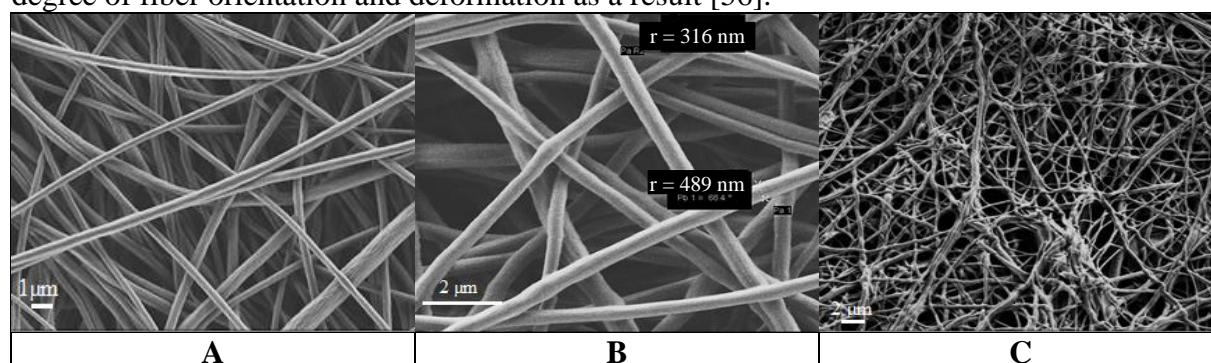

Figure 14: SEM images of cellulose after the different regeneration treatments. A. 28% NH_4OH solution for 4 days. B. 0.1 NaOH in ethanol. Diameter of the fibers is shown. C. 3.75 M NaOH + 2.1 M NaCl

5.1.2. Degree of regeneration

The FTIR method was used to analyze the changes in the chemical structure of CA after deacetylation. The main adsorption bands of the FTIR spectra of the pure CA are represented by stretching vibrations of the acetate substituent around 1745 cm^{-1} (C=O), 1375 cm^{-1} (C–CH$_3$), and 1235 cm^{-1} (C–O–C). Spectra of deacetylated samples are characterized by absence of C=O and C–O–C bands, while the C–CH$_3$ band is slightly visible (Fig. 15). At the same time the OH peak at 3500 cm^{-1} increased significantly, which points to complete deacetylation of samples treated both with NH$_4$OH and NaOH [57].
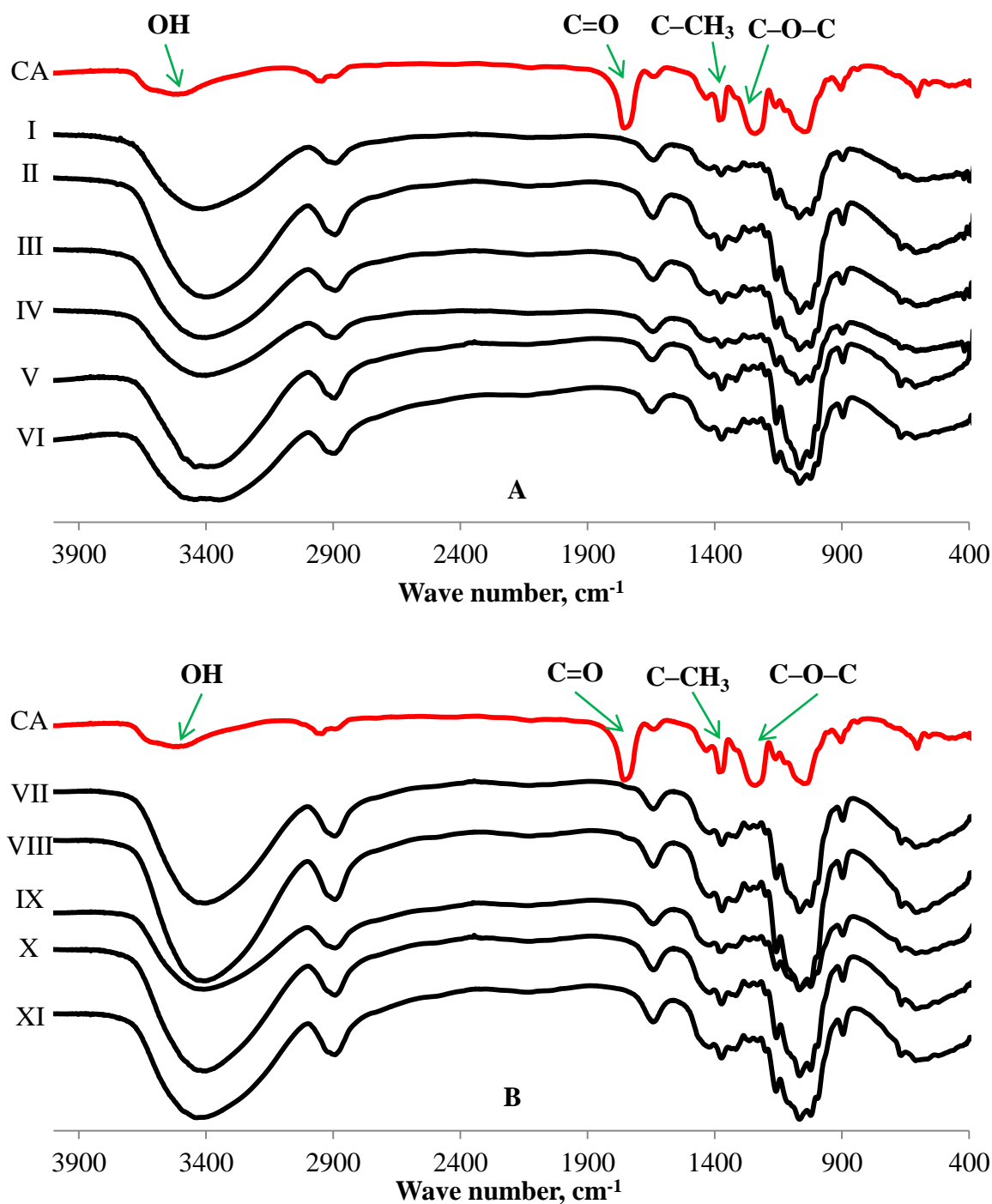
Figure 15: FTIR spectra of cellulose after the different deacetylation treatments.
A. NH$_4$OH. B. NaOH

5.1.3. Crystallinity

XRD patterns of deacetylated cellulose samples show the existence of three-dimensional order (crystalline parts) (Fig. 16). The crystal structure of cellulose II obtained after cellulose regeneration is assigned to peaks around 12° (101), 20° (10-1) and 22° (002). There are amorphous regions with lack of order as well. The ratio between crystalline and amorphous regions provides a nice opportunity to compare cellulose structures [58].
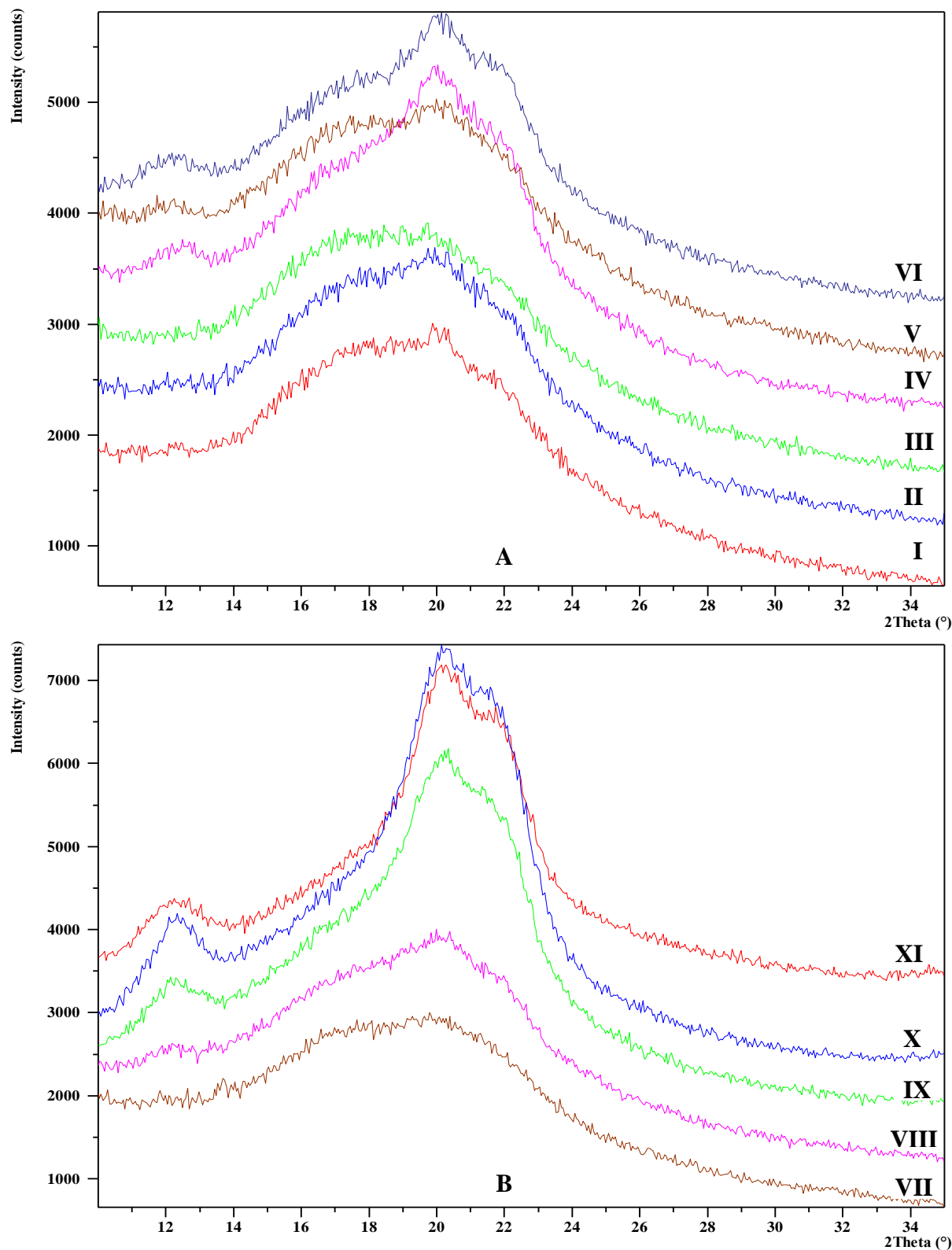

Figure 16: XRD patterns of the cellulose samples regenerated with A. NH_4OH; B. NaOH

Table 3: Crystallinity indices of the differently regenerated cellulose samples

Sample number	Crystallinity index, %
I	35
II	36
III	31
IV	44
V	32
VI	41
VII	34
VIII	40
IX	57
X	63
XI	66

In the case of NH_4OH the regeneration time proved to be an indecisive factor (Fig. 16A, Tab. 3). CI was in the range of 31-44% (accuracy ± 0.5%) and did not change in a monotonous way. XRD patterns of the samples regenerated in the presence of ethanol were characterized by better defined and resolved crystalline peaks. They had CI in the range of 36-44%, which is higher than CI of the samples regenerated without ethanol addition (32-35%). This can be explained by improved wettability of hydrophobic CA in water solution of NH_4OH, which led to more efficient deacetylation.

Cellulose samples regenerated with NaOH treatment were characterized by CI of 34-66% (Fig. 16B, Tab. 3). In the case of regeneration with NaOH the concentration of the regeneration agent is an important factor – the 0.1 M solution of NaOH contributes to a higher degree of cellulose crystallinity than the 0.05 M solution (Tab. 3). The influence of ethanol is noticeable as well. The samples regenerated in water solution of NaOH had CI 40% and 66%, while the samples regenerated in ethanol solution of NaOH had CI 34% and 57% for the two respective NaOH concentrations. This is probably due to a decreased hydrogen bonding capacity of ethanol in comparison to water, so it hinders cellulose molecules from close interaction with each other [55, 59]. Sample XI had the highest CI (66%), which could be due to the higher concentration of NaOH.

5.2. Carbon nanofibers

5.2.1. Morphology
Carbonization of EC samples resulted in flexible fibrous 25-40 μm thick mats. SEM gave information about the morphology of the carbon nanofibers produced (Fig. 17-19).

All the cellulose samples regenerated with NH_4OH, as well as the samples regenerated with 0.05 M NaOH, turned to be inappropriate precursors for CNF fabrication as the fibrous structure vanished during the carbonization. The fibers almost completely melted together; only at some areas the distinct fibers were observed (Fig. 17).

Fine fibers with granular structure were obtained from the cellulose regenerated with 0.1 M NaOH in ethanol or water; however cellulose regenerated with 3.75 M NaOH + 2.1 M NaCl did not result in smooth continuous fibers (Fig. 18-19). Basically the structures of the produced CNF resemble the structure of cellulose precursors (Fig. 14), except that the fiber diameter has decreased to 50-200 nm. So it is confirmed again that the fibrous structure was

not ruined during carbonization, remaining the same as after the regeneration process. The shrinkage of the fibers is correlated with the loss of mass [9].
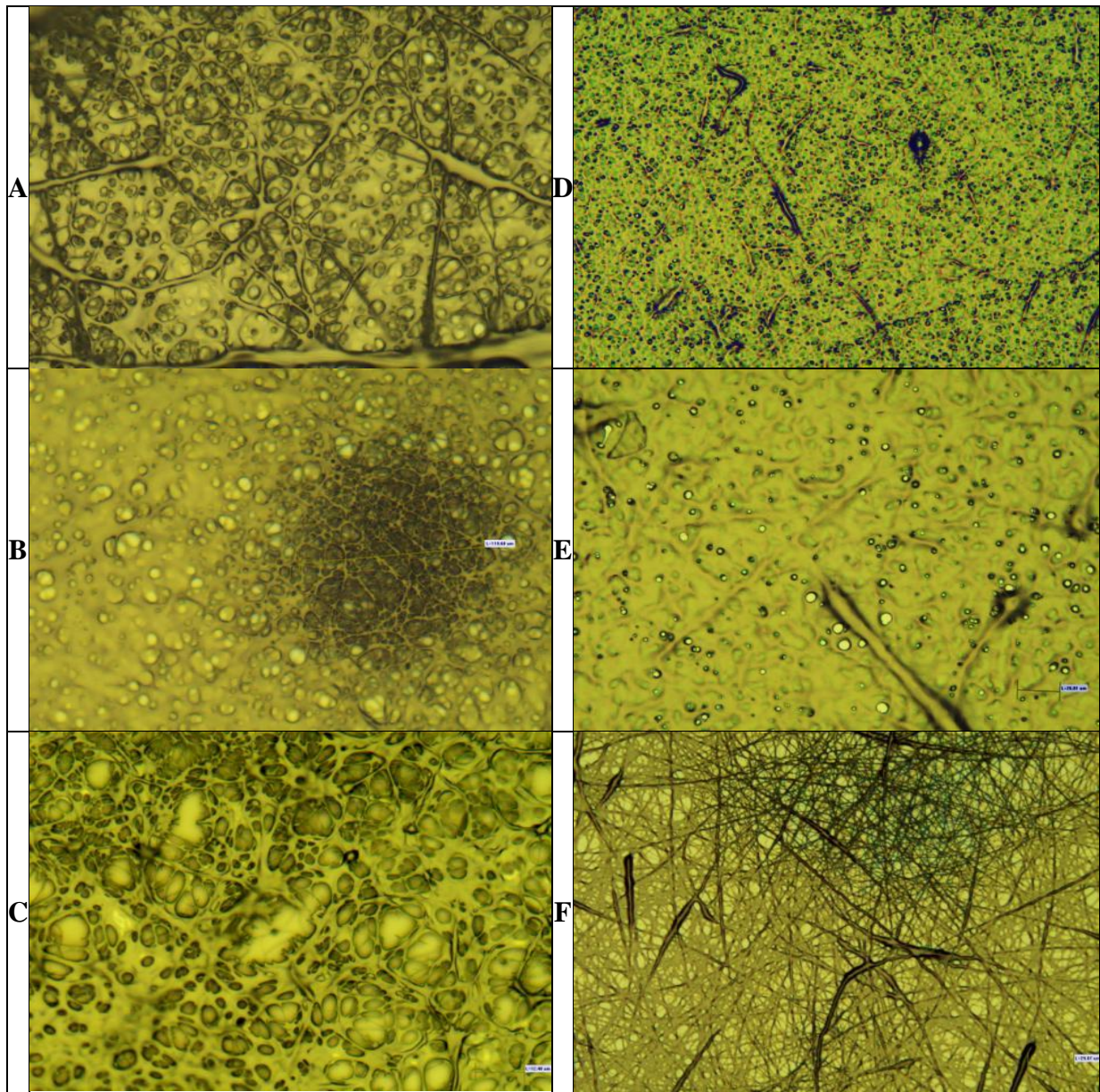

Figure 17: SEM images of the CNF synthesized from the cellulose carbonized at 800 °C. Cellulose was regenerated with A. 28% NH_4OH (4 days); B. 28% NH_4OH (8 days); C. 0.05 M NaOH in ethanol; D. 28% NH_4OH + ethanol (4 days); E. 28% NH_4OH + ethanol (4 days); F. 0.05 M NaOH in water
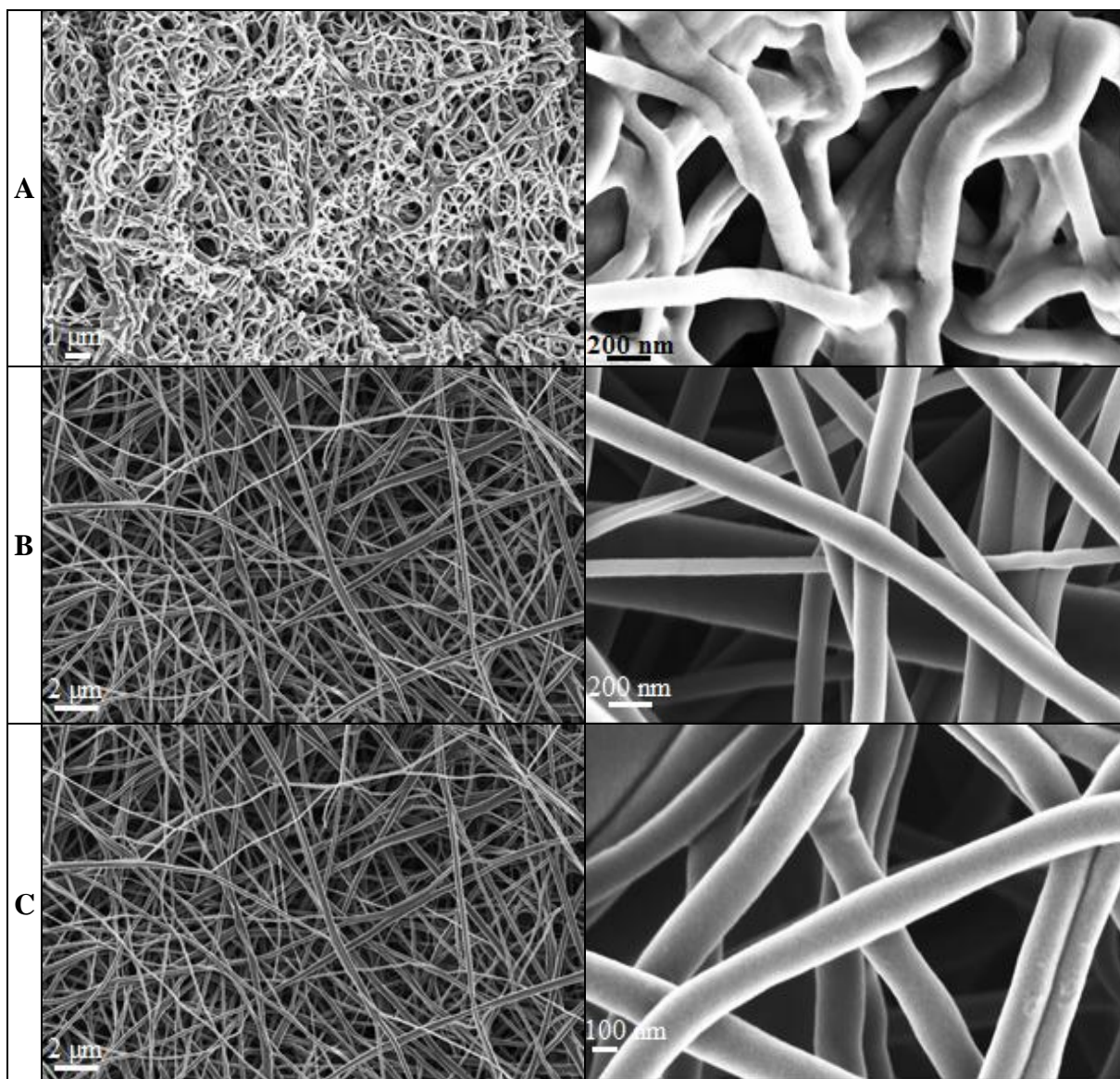
Figure 18: SEM images of the CNF synthesized from the cellulose carbonized at 800 °C. Cellulose was regenerated with A. 3.75 M NaOH + 2.1 M NaCl; B. 0.1 M NaOH in ethanol; C. 0.1 M NaOH in water

| A | B | C |

Figure 19: SEM images of granular structure of the CNF synthesized from the cellulose carbonized at 800 °C. Cellulose was regenerated with A. 3.75 M NaOH + 2.1 M NaCl; B. 0.1 M NaOH in ethanol; C. 0.1 M NaOH in water
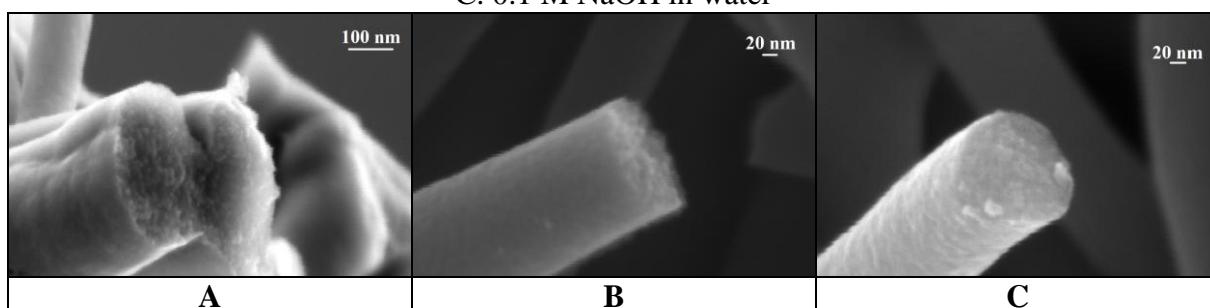
5.2.2. Decomposition during heating cycle

The samples that resulted in CNF production were evaluated with TGA. For TGA the same conditions were applied as for carbonization of cellulose to see the changes in weight related

to the temperature increase. The main loss was observed in the temperature range of 250-400 °C (Fig. 20). According to [9] it is due to the chain splitting dehydration that occurs in this temperature range (Fig. 9). The carbonization yield was calculated based on a theoretical carbon content in cellulose of 44.4 %. The carbon yield of the sample regenerated with 0.1 M NaOH in ethanol (IX) and in water (X) was 13% and 14%, respectively. The sample regenerated in highly concentrated NaOH (XI) gave a carbon yield of about 19%. These results correlate to the crystallinity indices of the mentioned samples. Samples with higher CI gave a higher carbon yield.
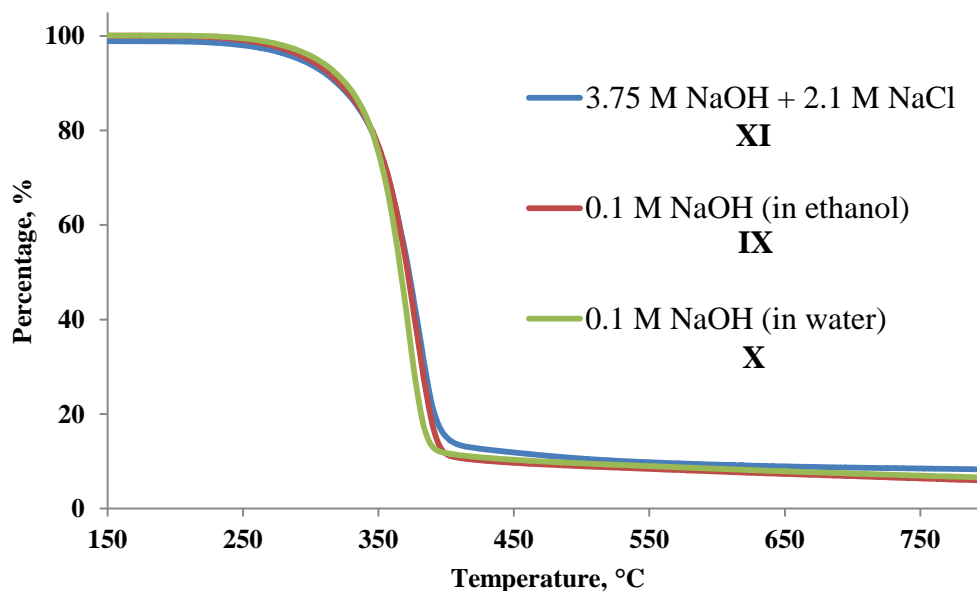

Figure 20: TGA of the cellulose regenerated with different methods

5.2.3. Chemical and elemental composition

With the help of XPS elemental composition as well as the chemical and valence state of the elements on the material surface were quantitatively measured, while EDS gave information about the elemental composition of a whole sample. In Tab. 4 C:O ratio of the CNF samples is shown.

Table 4: Elemental composition of CNF synthesized from differently deacetylated cellulose

Method of regeneration	Temperature of carbonization, °C	C:O atomic ratio (± 0.005)	
		Total	*Surface*
3.75 M NaOH + 2.1 M NaCl	800	46.61	21.36
0.1 M NaOH in ethanol	800	55.80	26.40
	1000	68.93	39.43
0.1 M NaOH in water	800	55.47	30.44
	1000	63.11	39.12

Obviously, the content of oxygen has decreased significantly after carbonization with the loss of H_2O and CO_2 predominantly [9]. Carbonization at 1000 °C has caused even larger evolution of these compounds from the structure, so the C:O ratio is higher than after carbonization at 800 °C. Samples of cellulose regenerated with 3.75 M NaOH + 2.1 M NaCl have resulted in totally different CNF with a greater oxygen content. For all the samples C:O

atomic ratio on the surface was higher than in total, since the surface is much more exposed to oxidation in the presence of O_2 traces and other oxidative species appearing during pyrolysis.

The surface of the carbonized samples consisted of only two chemical elements – carbon and oxygen. C1s spectra of carbon samples are shown in Figure 21. C1s spectra are asymmetric and broadened. They were resolved to several components which could be assigned to C–C (284.5 eV), C–O (around 288.8 eV), C=O or O–C–O (around 287 eV), and O–C=O (around 289 eV) [60]. It is worth to be noted that π–π*shake-ups were present in all the CNF samples (around 290 and 291.3 eV) indicating the emergence of sp^2 sites like in a graphitic structure [61].

Band	Pos	PosSep	%Area (± 0.005)
C–C	284.55	0.00	73.09
C–O	285.74	1.19	13.14
C=O	287.08	2.53	4.81
O–C=O	288.53	3.97	4.08
π–π*	290.06	5.51	2.71
π–π*	291.36	6.81	2.16
A			

Band	Pos	PosSep	%Area (± 0.005)
C–C	284.60	0.00	71.16
C–O	285.74	1.14	13.08
C=O	287.09	2.43	5.62
O–C=O	288.60	4.00	3.63
π–π*	290.07	5.47	3.63
π–π*	291.36	6.76	2.88
B			

Band	Pos	PosSep	%Area (± 0.005)
C–C	284.58	0.00	72.48
C–O	285.89	1.31	12.13
C=O	287.32	2.74	5.14
O–C=O	288.73	4.15	4.20
π–π*	290.21	5.64	3.20
π–π*	291.52	6.94	2.85
C			

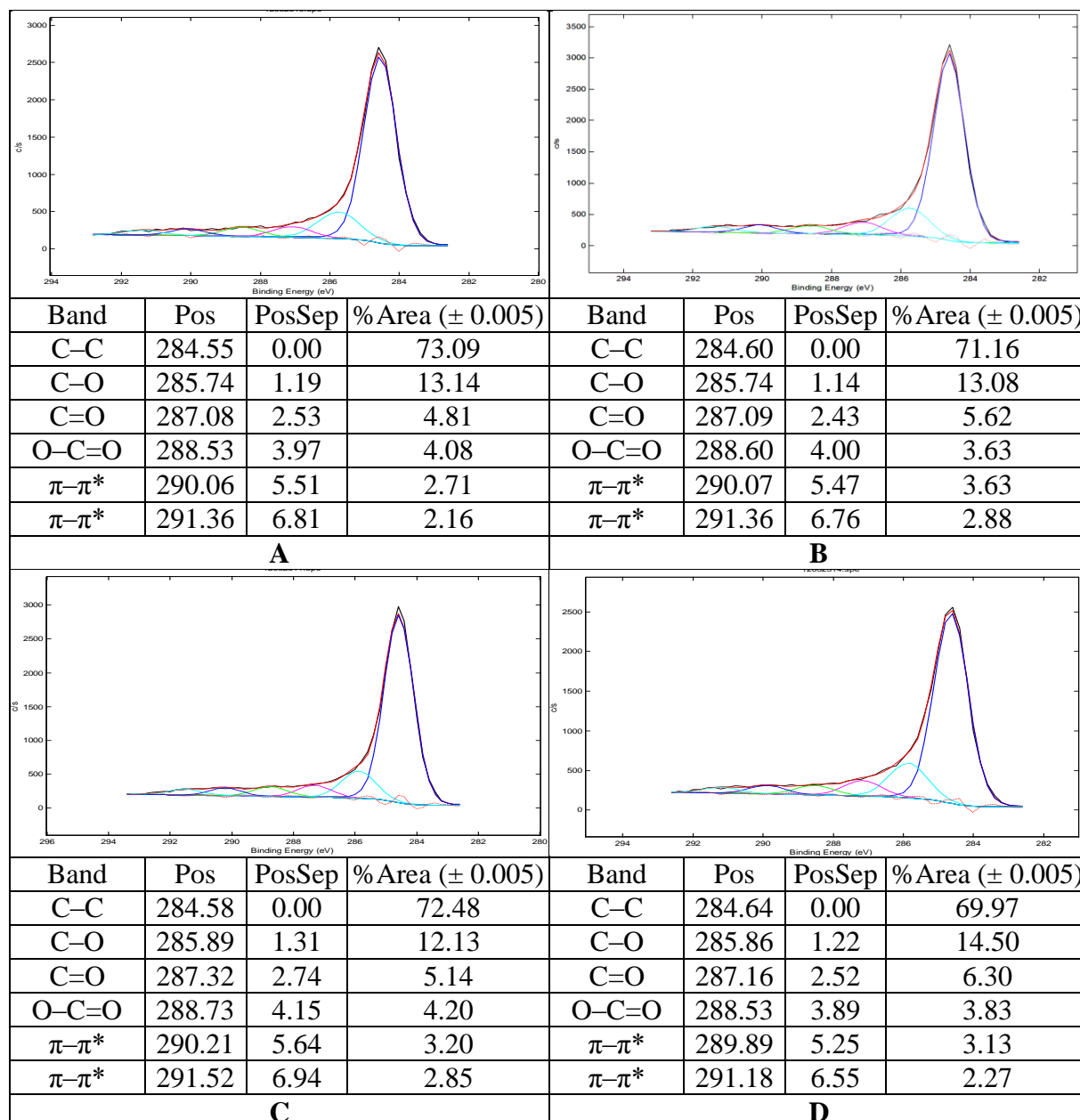| Band	Pos	PosSep	%Area (± 0.005)
C–C	284.64	0.00	69.97
C–O	285.86	1.22	14.50
C=O	287.16	2.52	6.30
O–C=O	288.53	3.89	3.83
π–π*	289.89	5.25	3.13
π–π*	291.18	6.55	2.27
D			

Figure 21: C1s spectra of the CNF obtained from the cellulose regenerated with: A. 0.1 M NaOH in ethanol (carbonized at 800 °C); B. 0.1 M NaOH in ethanol (carbonized at 1000 °C); C. 0.1 M NaOH in water (carbonized at 800 °C); D. 3.75 M NaOH + 2.1 M NaCl (carbonized at 800 °C)

5.2.4. Crystallinity

All the CNF synthesized from the regenerated cellulose had clearly amorphous structure (Fig. 22) which is typical for carbon materials synthesized by carbonization of cellulose at temperatures below 3000 °C [6].
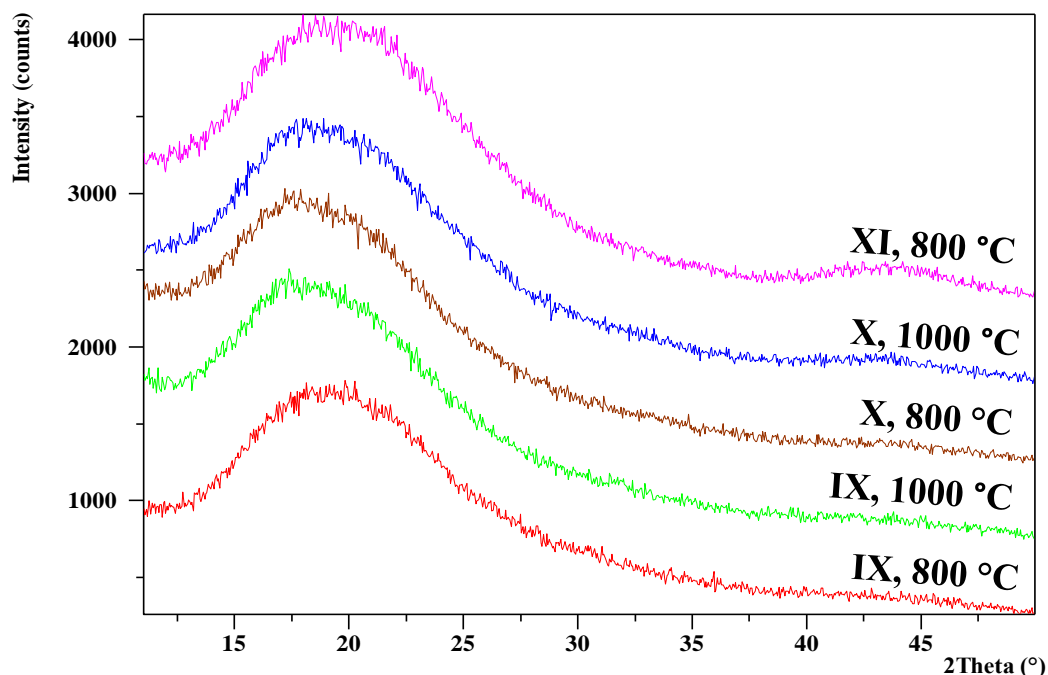

Figure 22: XRD patterns of the CNF synthesized from regenerated cellulose

5.2.5. Conductivity

The conductivity of CNF samples is in the range of 3.8-17.0 S/cm (accuracy ± 0.05 S/cm) which is comparable to semiconductive amorphous carbon [62]. Two factors that seem to have a definite impact on CNF conductivity are temperature of carbonization and method of cellulose regeneration (Tab. 5). The increase in conductivity after the carbonization at the higher temperature, 1000 °C, can be explained by the bigger C:O ratio in comparison with the carbonization at 800 °C (Tab. 4), while the relatively high conductivity of the CNF derived from the cellulose regenerated with 3.75 M NaOH + 2.1 M NaCl can be the result of a higher degree of interconnectivity of the fibers (Fig. 18A).
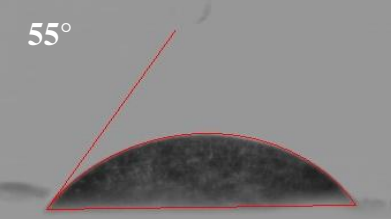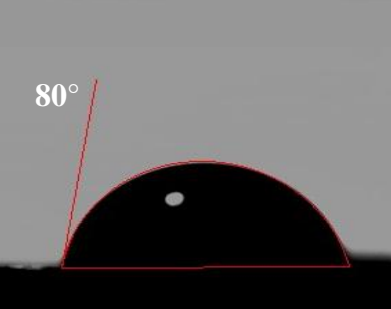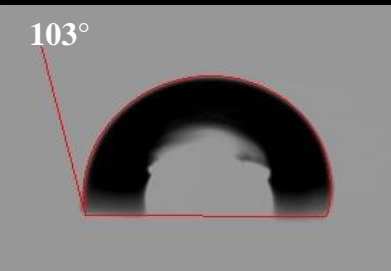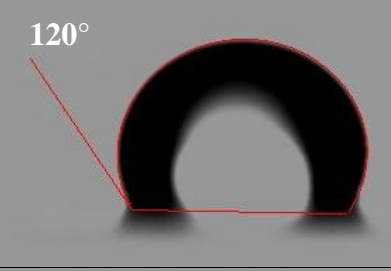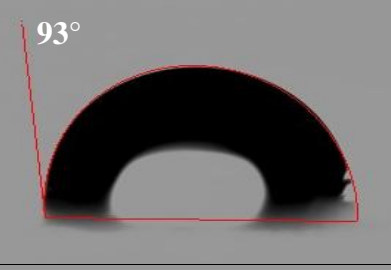
Table 5: Conductivity of CNF synthesized from the different precursors

Method of regeneration	*Temperature of carbonization, °C*	Conductivity, S/cm
3.75 M NaOH + 2.1 M NaCl	800	6.2
	1000	17.0
0.1 M NaOH in ethanol	800	3.8
	1000	10.0
0.1 M NaOH in water	800	4.5
	1000	10.1

5.2.6. Wettability

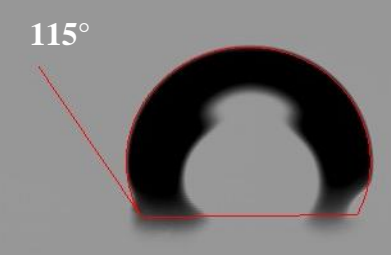To analyze the wettability of the different CNF samples, water contact angles were measured (Tab. 6).

Table 6: Wettability of CNF synthesized from the different precursors

Method of regeneration	Temperature of carbonization, °C	Contact angle
3.75 M NaOH + 2.1 M NaCl	800	**55°**
	1000	**80°**
0.1 M NaOH in ethanol	800	**103°**
	1000	**120°**
0.1 M NaOH in water	800	**93°**
	1000	**115°**

A general tendency of the material to become more hydrophobic with carbonization at higher temperature was observed, though all the samples regenerated with 0.1 M NaOH were

hydrophobic (103-120°). Most probably it was due to the change in C:O surface ratio mentioned above (Tab. 4) as the presence of polar oxygen atoms makes a surface attractive to the polar molecules of water, which results in lower contact angles. As we see, the lowest contact angle belonged to CNF produced from the cellulose regenerated with 3.75 M NaOH + 2.1 M NaCl (55°), and it perfectly corresponded to its low C:O value.

6. Conclusions

Carbon nanofibrous mats with fiber diameter of 50-200 nm were synthesized by carbonization of cellulose regenerated from electrospun cellulose acetate (with a carbon yield of up to 19%).

The samples with crystallinity indices in the range of 57-66 were appropriate for CNF production.

Carbonization led to the formation of amorphous CNF with the same morphology as the cellulosic precursors.

The obtained CNF had a conductivity of up to 17 S/cm which is comparable to semiconductive amorphous carbon.

CNF displayed a wide range of water contact angles (from 55º to 120º).

7. Plans for future work

Increasing the carbon yield together with the ability to carbonize non-fully regenerated samples of cellulose seem to be important goals for the future. Some substances (usually inorganic salts) can influence the cellulose carbonization procedure by lowering the degradation temperature and thus decreasing the degree of depolymerization of the cellulose. This effect can allow obtaining a higher carbon yield and also preserve the fibrous structure throughout the pyrolysis process. NH_4Cl will possibly be used to gain these advantages [9].

Evaluation of the other CNF properties (electrochemical, mechanical, thermoconductivity, surface area) can demonstrate the further opportunities to a great variety of different applications for this material. Good mechanical properties can provide utilization for CNF as reinforcement agent in composites; large surface area of CNF would be applicable in filters or separators in electronic devices.

Testing CNF as material for electrodes in supercapacitors and Li-ion batteries is foreseen to be the most attainable goal in the near future. CNF with a superb interconnectivity of pores, high mechanical strength and electrochemical stability can improve the performance of supercapacitors by increasing their capacity, cycle life, and decreasing the charging time.

Acknowledgements

References

[1]: De Jong K.P and Geus J. W (2000) Carbon nanofibers: Catalytic synthesis and applications. CATALYSIS REVIEWS – SCIENCE AND ENGINEERING, 42 (4), p. 481–510.

[2]: Greiner A and Wendorff J.H (2007) Electrospinning: A Fascinating Method for the Preparation of Ultrathin Fibers. ANGEW. CHEM. INT. ED., 46, p. 5670 – 5703.

[3]: Hedin N, Sobolev V, Zhang L, Zhu Z, Fong H (2011) Electrical properties of electrospun carbon nanofibers. J MATER SCI, 46 (19), p. 6453–6456.

[4]: Fang J, Niu H.T, Lin T and Wang X.G (2008) Applications of electrospun nanofibers. CHINESE SCIENCE BULLETIN, 15, p. 2265-2286.

[5]: Siro´ I, Plackett D (2010) Microfibrillated cellulose and new nanocomposite materials: a review. CELLULOSE, 17, p. 459-494.

[6]: Pierson H.O. Handbook of carbon, graphite, diamond, and fullerenes: properties, processing, and applications. Mill Road, NJ: Noyes Publications, 1993.

[7]: Upadhyayula V.K.K, Meyer D.E, Curran M.A, Gonzalez M.A (2012) Life cycle assessment as a tool to enhance the environmental performance of carbon nanotube products: a review. J. CLEANER PRODUCTION, 26, p. 37-47.

[8]:http://www.opg.com/power/thermal/Pembina%20Biomass%20Sustainability%20Analysis%20Summary%20Report.pdf.

[9]: Morgan P. Carbon fibers and their composites. Boca Raton, FL: Taylor & Francis Group, 2003.

[10]: Inagaki M. New carbons - control of structure and functions. Elsevier, 2000.

[11]: Ghavanini F.A, Lopez-Damian M, Rafieian D, Svensson K, Lundgren P, Enoksson P (2011) Controlling the initial phase of PECVD growth of vertically aligned carbon nanofibers on TiN. SENSORS AND ACTUATORS A, 172, p. 347– 358.

[12]: Khanna V, Bakshi B.R, and Lee L.J (2008) Carbon Nanofiber Production: Life Cycle Energy Consumption and Environmental Impact. JOURNAL OF INDUSTRIAL ECOLOGY, 12 (3), p. 394-410.

[13]: McKnight T.E., Melechko A.V, Hensley D.K, Mann D.G.J, Griffin G.D, and Simpson M.L (2004) Tracking gene expression after DNA delivery using spatially indexed nanofiber arrays. NANO LETTERS, 4(7), p. 1213-1219.

[14]: Price R.L, Waid M.C, Haberstroh K.M, Webster T.J (2003) Selective bone cell adhesion on formulations containing carbon nanofibers. BIOMATERIALS, 24, p. 1877–1887.

[15]: Tungprapa S, Puangparn T, Weerasombut M, Jangchud I, Fakum P, Semongkhol S, Meechaisue C, Supaphol P (2007) Electrospun cellulose acetate fibers: effect of solvent system on morphology and fiber diameter. CELLULOSE, 14, p. 563–575.

[16]:Kang K.S, Cho K.Y, Lim H.K and Kim J (2008) Investigation of surface morphology of cellulose acetate micro-mould after deacetylation. JOURNAL OF PHYSICS D: APPLIED PHYSICS, 41, p. 1-5.

[17]: Oh S.Y, Yoo D.I, Shin Y, Kim H.C, Kim H.Y, Chung Y.S, Park W.H, Youk J.H (2005) Crystalline structure analysis of cellulose treated with sodium hydroxide and carbon dioxide by means of X-ray diffraction and FTIR spectroscopy. CARBOHYDRATE RESEARCH, 340 (15), p. 2376–2391.

[18]: Fischer S, Thűmmler K, Volkert B, Hettrich K, Schmidt I and Fischer K (2008) Properties and applications of cellulose acetate. MACROMOL. SYMP., 262, p. 89–96.

[19]: Hajji F (2011) Engineering renewable cellulosic thermoplastics. REV ENVIRON SCI BIOTECHNOL, 10, p. 25-30.

[20]: Inagaki M, Park K.C, Endo M (2010) Carbonization under pressure. NEW CARBON MATERIALS, 25(6), p. 409-420.

[21]: Teo W.E, Ramakrishna S (2006) A review on electrospinning design and nanofibre assemblies. NANOTECHNOLOGY, 17, p. 89-106.

[22]: Park J.S (2010) Electrospinning and its applications. ADV. NAT. SCI.: NANOSCI. NANOTECHNOL., 1, p. 1-5.

[23]: Doshi J, Reneker D.H (1995). Electrospinning process and applications of electrospun fibers. J ELECTROSTATICS, 35 (2-3), p. 151-160.

[24]: Reneker D.H, Chun I.S (1996), Nanometre diameter fibres of polymer, produced by electrospinning. NANOTECHNOLOGY, 7, p. 216-223.

[25]: Gibson P, Schreuder-Gibson H, Rivin D (2001), Transport properties of porous membranes based on electrospun nanofibers. COLLOIDS SURF A, 187-188, p. 469-481.

[26]: Pham Q.P, Sharma U and Mikos A.G (2006) Electrospinning of Polymeric Nanofibers for Tissue Engineering Applications: A Review. TISSUE ENGINEERING, 12 (5), p. 1197-1211.

[27]: Ki C.S, Baek D.H, Gang K.D, Lee K.H, Um I.C and Park Y.H (2005) Characterization of gelatin nanofiber prepared from gelatin-formic acid solution. POLYMER, 46 (14), p. 5094-5102.

[28]: Deitzel J.M, Kleinmeyer J, Harris D and Tan N.C.B (2001) The effect of processing variables on the morphology of electrospun nanofibers and textiles. POLYMER, 42 (1), p. 261-272.

[29]: Fong H, Chun I and Reneker D.H (1999) Beaded nanofibers formed during electrospinning. POLYMER, 40 (16), p. 4585-4592.

[30]: Demir M.M, Yilgor I, Yilgor E and Erman B (2002) Electrospinning of polyurethane fibers. POLYMER, 43 (11), p. 3303-3309.

[31]: Zong X.H, Kim K, Fang D.F, Ran S.F, Hsiao B.S and Chu B (2002) Structure and process relationship of electrospun bioabsorbable nanofiber membranes. POLYMER, 43 (16), p. 4403-4412.

[32]: Mckee M.G, Wilkes G.L, Colby R.H and Long T.E (2004) Correlations of solution rheology with electrospun fiber formation of linear and branched polyesters. MACROMOLECULES, 37 (5), p. 1760-1767.

[33]: Liu H.Q and Hsieh Y.L (2002) Ultrafine fibrous cellulose membranes from electrospinning of cellulose acetate. J. POLYM. SCI. B-POLYM. PHYS., 40 (18), p. 2119-2129.

[34]: Jiang H.L, Fang D.F, Hsiao B.S, Chu B and Chen W.L (2004) Optimization and characterization of dextran membranes prepared by electrospinning. BIOMACROMOLECULES, 5 (2), p. 326-333.

[35]: Mit-uppatham C, Nithitanakul M and Supaphol P (2004) Ultrafine electrospun polyamide-6 fibers: effect of solution conditions on morphology and average fiber diameter. MACROMOL. CHEM. PHYS., 205 (17), p. 2327-2338.

[36]: Zuo W.W, Zhu M.F, Yang W, Yu H, Chen Y.M and Zhang Y (2005) Experimental study on relationship between jet instability and formation of beaded fibers during electrospinning. POLYM. ENG. SCI., 45 (5), p. 704-709.

[37]: Lin T, Wang H.X, Wang H.M and Wang X.G (2004) The charge effect of cationic surfactants on the elimination of fibre beads in the electrospinning of polystyrene. NANOTECHNOLOGY, 15 (9), p. 1375-1381.

[38]: Zhang C.X, Yuan X.Y, Wu L.L, Han Y and Sheng J (2005) Study on morphology of electrospun poly(vinyl alcohol) mats. EUR. POLYM. J., 41 (3), p. 423-432.

[39]: Geng X.Y, Kwon O.H and Jang J.H (2005) Electrospinning of chitosan dissolved in concentrated acetic acid solution. BIOMATERIALS, 26 (27), p. 5427-5432.

[40]: Li D and Xia Y.N (2004) Direct fabrication of composite and ceramic hollow nanofibers by electrospinning. NANO. LETT., 4 (5), p. 933-938.

[41]: Ding B, Kimura E, Sato T, Fujita and Shiratori S (2004) Fabrication of blend biodegradable nanofibrous nonwoven mats via multi-jet electrospinning. POLYMER, 45 (6), p. 1895-1902.

[42]: Kim H.S, Kim K, Jin H.J and Chin I.J (2005) Morphological characterization of electrospun nano-fibrous membranes of biodegradable poly(L-lactide) and poly(lactideco-glycolide). MACROMOL. SYMP., 224 (1), p. 145-154.

[43]: Matthews J.A, Wnek G.E, Simpson D.G and Bowlin G.L (2002) Electrospinning of collagen nanofibers. BIOMACROMOLECULES, 3 (2), p. 232-238.

[44]: Dalton P.D, Klee D and Moller M (2005) Electrospinning with dual collection rings. POLYMER, 46 (3), p. 611-614.

[45]: Deitzel J.M, Kleinmeyer J.D, Hirvonen J.K and Tan N.C.B (2001) Controlled deposition of electrospun poly(ethylene oxide) fibers. POLYMER, 42 (19), p. 8163-8170.

[46]: Casper C.L, Stephens J.S, Tassi N.G, Chase D.B and Rabolt J.F (2004) Controlling surface morphology of electrospun polystyrene fibers: effect of humidity and molecular weight in the electrospinning process. MACROMOLECULES, 37 (2), p. 573-578.

[47]: Lee K.Y, Jeong L, Kang Y.O, Lee S.J and Park W.H (2009) Electrospinning of polysaccharides for regenerative medicine. ADVANCED DRUG DELIVERY REVIEWS, 61, p. 1020-1032.

[48]: Zhang L, Menkhaus T.J, Fong H (2008) Fabrication and bioseparation studies of adsorptive membranes/felts made from electrospun cellulose acetate nanofibers. J. MEMBR. SCI., 319 (1), p. 176–184.

[49]: Kim C, Frey M.W, Marquez M, Joo Y.L (2005) Preparation of submicron-scale, electrospun cellulose fiber via direct dissolution. J. POLYM. SCI. POLYM. PHYS., 43 (13), p. 1673–1683.

[50]: Kim C, Kim D, Kang S, Marquez M, Joo Y.L (2006) Structural studies of electrospun cellulose nanofibers. POLYMER, 47 (14), p. 5097–5107.

[51]: Kulpinski P (2005) Cellulose nanofibers prepared by the N-methylmorpholine-N-oxide method. J. APPL. POLYM. SCI., 98, p. 1473–1482.

[52]: Han S.O, Son W.K, Youk J.H, Park W.H (2008) Electrospinning of ultrafine cellulose fibers and fabrication of poly(butylene succinate) biocomposites reinforced by them. J. APPL. POLYM. SCI., 107 (3), p. 1954–1959.

[53]: Jarusuwannapoom T, Hongrojjanawiwat W, Jitjaicham S, Wannatong L, Nithitanakul M, Pattamaprom C, Koombhongse P, Rangkupan R, Supaphol P (2005) Effect of solvents on electro-spinnability of polystyrene solutions and morphological appearance of resulting electrospun polystyrene fibers. EUR POLYM J, 41 (3), p. 409–421.

[54]: Pattamaprom C, Hongrojjanawiwat W, Koombhongse P, Supaphol P, Jarusuwannapoom T, Rangkupan R (2006) The influence of solvent properties and functionality on the electrospinnability of polystyrene nanofibers. MACROMOL MATER ENG, 291 (7), p. 840–847.

[55]: Buschle-Diller G and Zeronian S.H (1992) Enhancing the reactivity and strength of cotton fibers. JOURNAL OF APPLIED POLYMER SCIENCE, 45, p. 967-979.

[56]: Nikitin V et al. The chemistry of wood and cellulose. Moscow: Forest Industry, 1978.

[57]: Son W.K, Youk J.H, Lee T.S, Park W.H (2004) Electrospinning of ultrafine cellulose acetate fibers: studies of a new solvent system and deacetylation of ultrafine cellulose acetate fibers. JOURNAL OF POLYMER SCIENCE: PART B: POLYMER PHYSICS, 42, p. 5–11.

[58]: Fink H.P, Hofmann D, Philipp B (1995) Some aspects of lateral chain order in cellulosics from X-ray scattering. CELLULOSE, 2, p. 51-70.

[59]: Zeronian S.H (1970) Acetylation of cotton treated with sodium hydroxide. JOURNAL OF APPLIED POLYMER SCIENCE, 14, p. 365-372.

[60]: Rhim Y-R et al. (2010) Changes in electrical and microstructural properties of microcristalline cellulose as function of carbonization temperature. CARBON, 48, p. 1012-1024.

[61]: Gaskell P.H, Saeed A, Chieux P, McKenzie D.R (1991) Neutron diffraction studies of the structure of highly tetrahedral amorphous diamond-like carbon. PHYS REV LETT, 67, p. 1286-1289.

[62]: Serway R.A. and Jewett J.W. Principles of physics. Belmont, Calif.: Thompson/Brooks/Cole, 2006.

Paper

Carbon nanofibers with controlled properties synthesized from electrospun cellulose.
O. Naboka, V. Kuzmenko, A. Sanz-Velasco, P. Lundgren, P. Enoksson, P. Gatenholm.
Carbon 2012, *The Annual World Conference on Carbon*, *Krakow, Poland, June 17-22, 2012.*

CARBON NANOFIBERS WITH CONTROLLED PROPERTIES SYNTHESIZED FROM ELECTROSPUN CELLULOSE

Olga Naboka [1,2], Volodymyr Kuzmenko[1,2], Anke Sanz-Velasco[1,2], Per Lundgren[1,2], Peter Enoksson[1,2], Paul Gatenholm[2,3]

[1]Department of Microtechnology and Nanoscience, Chalmers University of Technology SE-412 96, Gothenburg, Sweden
[2]Wallenberg Wood Science Center, Chalmers University of Technology SE-412 96, Gothenburg, Sweden
Department of Chemical and Biological Engineering,
[3]Chalmers University of Technology SE-412 96, Gothenburg, Sweden

Introduction

It is difficult to overestimate the importance of low-dimensional carbon materials for present and future applications. Energy conversion, functional composites, field emitters, sensors and drug delivery are just a few examples of prospective applications for carbon nanostructures [1].

Presently environmental impact of carbon nanostructures is considered to be of the same importance as possibility of large scale production of carbon nanomaterials with controllable properties [2]. Replacement of raw materials of fossil origin with renewable plant derived materials could contribute significantly to the improvement of environmental performance of nanocarbon products [2].

Cellulose as the most abundant natural polymer [3] is seen to be the inexhaustible source for the synthesis of various carbon nanomaterials. Main drawbacks of cellulose are wide distribution of properties depending on the plant source and processing conditions [3] and low carbonization yield [4]. While for fabrication of bulk carbon materials impact of cellulose crystal state and molecular weight could be neglected to some extend properties of synthesized carbon nanostructures could be considerably affected by differences in precursor used.

Some works were conducted to investigate the influence of cellulosic precursor on its pyrolysis [5, 6] but samples chosen for comparision differed by several parameters such as origin, type of crystal structure etc. which in our opinion makes it difficult to differentiate influence of each factor on the process.

Aim of our work was synthesis of carbon nanofibrous materials by carbonization of cellulose regenerated from electrospun cellulose acetate and investigation of influence of crystallinity of cellulose on the carbon formed.

Experimental

Cellulose acetate (CA) with Mn~30,000 and 39.9 wt% acetyl content (Aldrich), NaOH NaCl, (analytical grade, Riedel-de-Haën), acetone (analytical grade, Solveco), ethanol (analytical grade, Solveco), dimethylacetamide (99.9%, Sigma Aldrich) were used as received without additional purification.

Electrospinning of CA. Fibrous mats were produced by electrospinning of CA. CA solution of 17% Wt/Wt in acetone/dimethylacetamide 2:1 ratio was used at 22°C and 60% of relative humidity. CA solution was fed at 1 ml/h through a stainless steel needle with a diameter of 0.643 mm at 25 kV applied voltage. The distance between needle and collector was 25 cm.

Regeneration to Cellulose (EC) was performed by three methods of alkaline treatment of electrospun fibrous mats:

- in the 0.1M solution of NaOH in ethanol for 24 hours (ECet);
- in the 0.1M solution of NaOH in water for 24 hours (ECaq);
- in the water solution of NaOH/NaCl (3.75M NaOH, 2.1M NaCl [7]) during 2 hours at 65°C. 2 ml of ethanol was added to each 100 ml of solution in order to improve wetting of CA (ECf)

Regenerated EC sheets were rinsed and kept overnight in deionized water. Drying was carried out on air in polystyrene Petri dishes.

The **carbonization of EC samples** placed between silicon wafers was carried out in a quartz tube furnace Tempress in N_2 flow by heating up to 800 and 1000 with the heating rate of 5°C/min. Samples were kept at the highest temperature for 2 hours before cooling down.

Scanning Electron Microscopy (SEM) was performed with Leo Ultra 55 FEG SEM (Zeiss) at the acceleration voltage in the range of 1.0 to2.5 kV.

Fourier-Transform Infrared (FTIR) Spectroscopy was performed with Perkin Elmer System 2000 FT-IR spectrometer in 4000-370 cm^{-1} in transmission mode. Spectra were recorded using tablets prepared from 0.5 mg of EC and 100.0 mg of KBr.

X-Ray Diffraction Analysis (XRD) was carried out with Philips X'Pert Materials Research Diffractometer (MRD). Radiation was generated with an X-ray tube with Cu anode (Kα radiation, λ=1.54184 Å) at 45 kV and 40 mA. The 2θ range was 10-37°, and the resolution was 0.05° with 30 seconds averaging time per step. Crystallinity index (CrI) of EC was determined as in Eq. (1) [8]:

$$CrI = 1 - I1/I2 \qquad (1)$$

Where I1 is the intensity at the minimum around 2θ=13,8°, I2 is the intensity of the peak at 2θ=20,2°.

Raman Spectroscopy was carried out with the LabRam (Horiba) Raman spectrometer, equipped with Ar laser (514.5 nm). Analysis of spectra was made with Origin 7.5 software.

Thermogravimetric Analysis was performed with Pyris TGA 7 (Perkin Elmer) in the N_2 flow in the temperature range from 105°C to 800°C with the heating rate 5°C/min.

Carbonization yield was calculated based on theoretical carbon content in cellulose of 44.4 %.

Results and Discussion

Electrospinning of CA solutions leads to formation of flexible fibrous mats with thickness of 60-90 μm consisting of fibers of 0.3-1.5 μm in diameter (fig.1).
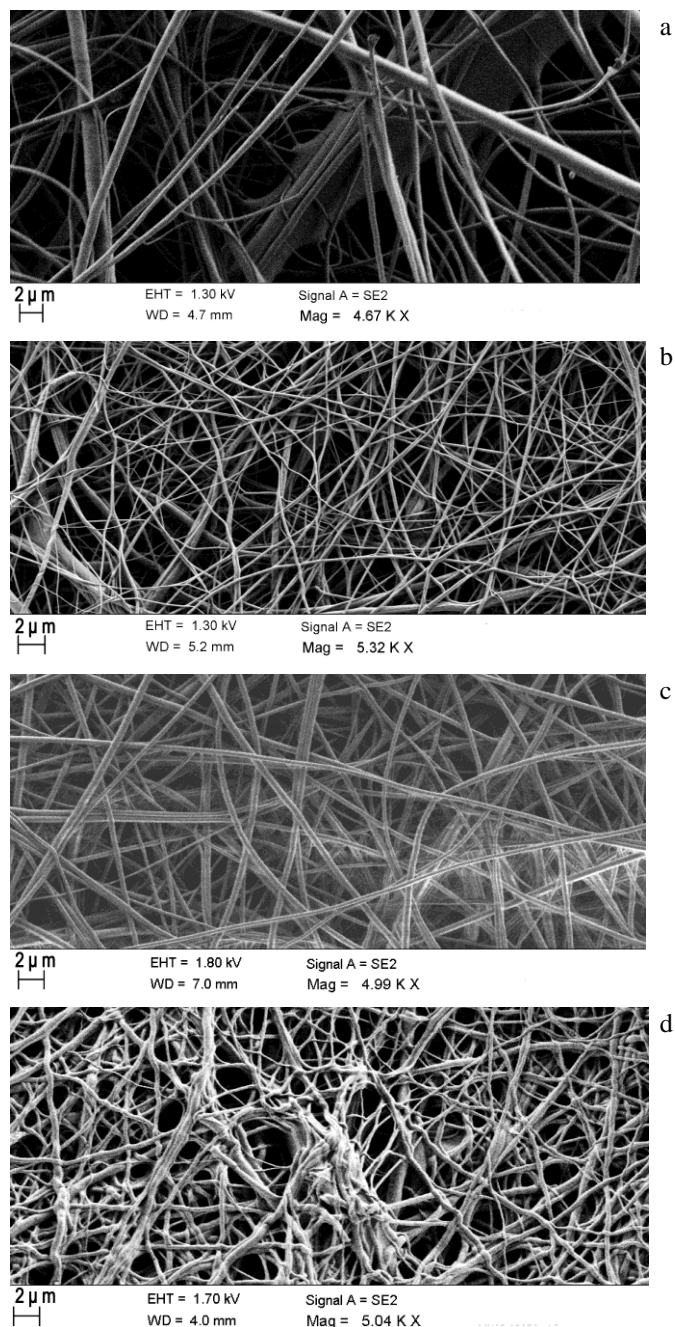

Fig.1 SEM images of electrospun CA (a) and regenerated cellulose ECet (b), ECaq (c), ECf (d).

Regenerated ECet and ECaq retain the morphology of electrospun CA. Structure of ECf is deformed to a large extend most likely because of the swelling of cellulose during the treatment in hot concentrated alkaline solution (fig.1).

FTIR spectra of regenerated cellulose (not shown here) differ from FTIR spectra of starting electrospun CA by the absence of peaks assigned to stretching vibrations of C=O (1756 cm^{-1}) and alkoxyl stretch of C-O-C (1241 cm^{-1}) from ester groups and significant broadening of the hydroxyl peak (3400 cm^{-1}) [9] which points to complete deacetylation of CA.

XRD patterns of EC samples have peaks around 12°, 20° and 22°(fig. 2) which is typical for XRD patterns of cellulose II [10].
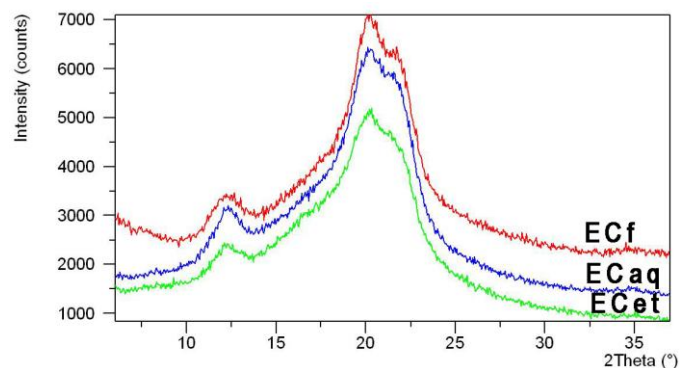
Fig.2 XRD patterns of EC samples

It was found that EC samples differ by crystallinity index: ECf is characerized by the highest CrI (0.67) and ECet has the lowest CrI=0.57 (table 1). Results obtained could be explained not only by influence of concentration and temperature of NaOH solution used for the deacetylation of CA (as for samples ECf and ECaq) but also by the influence of dispersion medium (water or ethanol) used to dissolve NaOH [8]. Ethanol having ability to form only one hydrogen bond per molecule does not allow cellulose to form interchain hydrogen bond which results in lower crystallinity index [8].

Table 1. Yield and the I_D/I_G of Carbon Samples synthesized from EC at 800°C

sample	CrI of cellulose	Yield of carbon at 800°C, %	I_D/I_G of carbons synthesized at 800°C
ECet	0.58	13	1.64
ECaq	0.63	15	1.39
ECf	0.67	19	1.16

Carbonized EC samples are flexible fibrous mats with thickness of 25-40 μm.

Despite some shrinkage of EC samples occurs during carbonization carbon materials synthesized retain the fibrous morphology of starting EC samples –straight fibers were

received from ECet (fig. 3a) and ECaq (fig. 3b), twisted and fused together fibers were formed from ECf (fig. 3c).
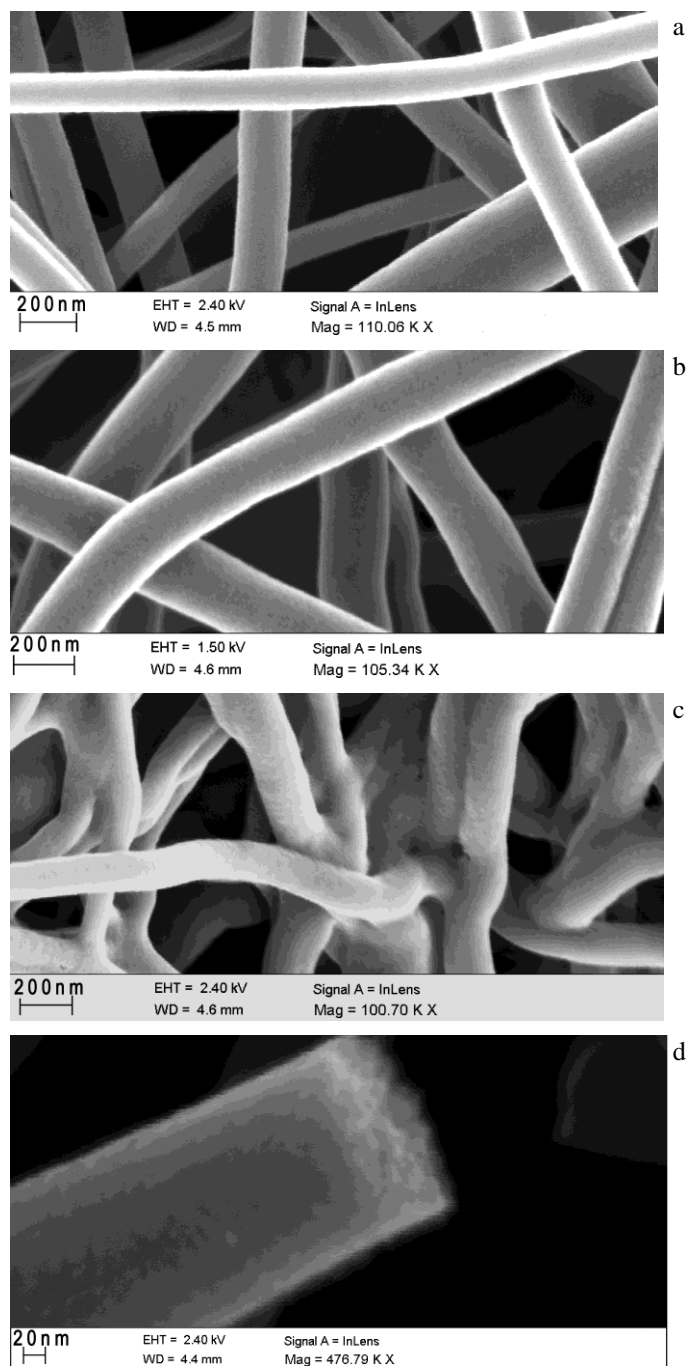
Fig.3 SEM images of carbon nanofibers synthesized at 800°C from ECet (a,d), ECaq (b), ECf (c).

Diameter of carbon fibers was in range of 50-300 nm (fig.3 a-c). Fibers received from all EC samples show the same granular microstructure with the average grain size of 8-12 nm (fig. 3d) similar to that observed in [11]

Raman spectra of samples have two froad complex peaks centered around 1355 cm^{-1} (D-band) and 1585 cm^{-1} (G-band) typical for amorphous carbon [12]. Deconvolution of these peaks reveals the presence of five peaks centered at 1130, 1355, 1485, 1585, 1620 cm^{-1}. Example of deconvoluted Raman spectrum is shown on fig. 4. for the carbon synthesized from ECf. G band could be assigned to the in-plane vibrations of the sp^2-bonded crystallite carbon and D-band is could be assigned to in-plane vibrations of the sp^2-bonded carbon in structural defects [12].
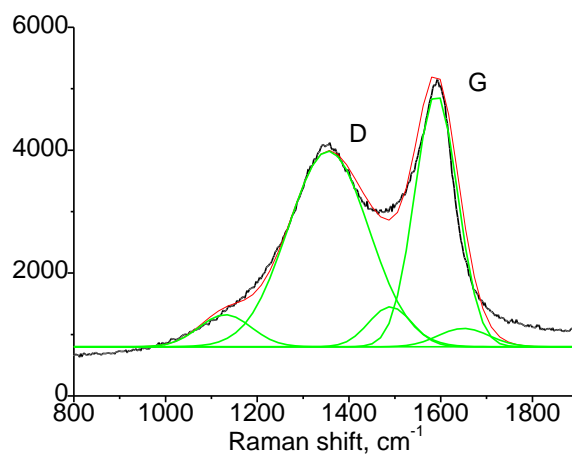
Fig.4 Raman spectrum of carbon synthesized by the carbonization of ECf.

The ratio of the integrated areas of deconvoluted D-band and G-band (I_D/I_G) is commonly used to evaluate the degree of the structural organization of synthesized carbons, the lower I_D/I_G the higher content of ordered sp^2 carbon crystallites [12, 13]. It was revealed that Raman spectrum of carbon originated from the ECf has the lowest I_D/I_G – 1.16, the spectrum of ECet is characterized by the highest I_D/I_G of 1.64. (table 1). Thus microstructure of carbon synthesized at 800° correlates to crystallinity of cellulosic precursor.

Thermogravimetric analysis was performed in order to investigate influence of the starting cellulose on carbonization yield. According to TGA sample possessing the highest crystallinity index (ECf) gives the highest carbonization yield (19%) while the lowest yield (13%) was received from carbonization of ECet which has the lowest crystallinity index.

Taking into account that the same CA precursor was used to produce cellulose, alkaline deacetylation was perfoemed with the same reagent (NaOH), rinsing and drying conditions for regenerated cellulose were maintained to be the same one

could conclude that changes in carbonization yield and carbon microstructure are connected to the degree of crystallinity of precursor cellulose.

Conclusions

Flexible carbon nanofibrous mats consisting of amorphous nanofibers was synthesized by carbonization of fibrous cellulose regenerated from electrospun cellulose acetate at 800°C in nitrogen flow. According to SEM carbonization of cellulose with fiber diameter of 0.3-1.5 μm led to formation of granular fibrillar carbon with fiber diameter of 50-300 nm. It was shown that crystallinity index of starting cellulose affects both carbonization yield and carbon structure. The higher crystallinity index resulted in the higher carbonization yield and in the higher degree of structural organization of carbon formed.

References

[1] L. Dai [ed], Carbon nanotechnology: recent developments in chemistry, physics, materials science and device applications. Amsterdam, Boston: Elsevier B. V; 2006.
[2] Upadhyayula VKK, Meyer DE, Curran MA, Gonzalez MA. Life cycle assessment as a tool to enhance the environmental performance of carbon nanotube products: a review. J. Cleaner Production 2012;26:37-47.
[3] Klemm D, Heublein B, Fink HP, Bohn A. Cellulose: fascinating biopolymer and sustainable raw material. Angew. Chem. Int. Ed. 2005;44:3358-3393.
[4] Paris O, Zollfrank C, Zickler GA. Decomposition and carbonization of wood biopolymers – a microstructural study of softwood pyrolysis. Carbon 2005;43:53-66.
[5] Zhang J, Luo J, Tong D, Zhu L, Dong L, Hu C. The dependence of pyrolysis behavior on the crystal state of cellulose. Carbohydrate Polymers 2010;79:164-169.
[6] Poletto M, Pistor V, Zeni M, Zattera AJ. Crystalline properties and decomposition kinetics of cellulose fibers in wood pulp obtained by two pulping processes. Polymer Degradation and Stabiity 2011;96:679-685.
[7] Bakunov VA, Budnitskii GA, Maiboroda LF. Hollow cellulose acetate fibres for hemodialysis. Khimicheskie Volokna 1979;(6):30-32.
[8] Buschle-Diller G, Zeronian SH. Enhancing the reactivity and strength of cotton fibers. J. Appl. Polym. Sci. 1992;45:967-979.
[9] Chen Y, Xiong XP, Yang G. Characterization of regenerated cellulose membranes hydrolysed from cellulose acetate. Chinese J. Polym. Sci. 2002;20:369-375.
[10] Fink et al., 1995
[11] Hishiyama Y, Yoshida A, Kaburagi Y. Resistivity, Hall coefficient, magnetoresistance, and microtexture of cellulose carbon films. Carbon 1993;31:1265-1272.
[12] Rhim YR, Zhang D, Fairbrother DH, Wepasnick KA, Livi KJ, Bodnar RJ, Nagle DC. Changes in electrical and microstructural properties of microcrystalline cellulose as function of carbonization temperature. Carbon 2010;48:1012-1024.

[13] Ruiz-Rosas R, Bedia J, Lallave M, Loscertales IG, Barrero A, Rodriguez-Mirasol J, Cordero T. The production of submicron diameter carbon fibers by the electrospinning of lignin. Carbon 2010;48:696-705.